Quantized response and topology of magnetic insulators with inversion symmetry

Ari M. Turner, Yi Zhang, Roger S. K. Mong, and Ashvin Vishwanath

Quantized Response and Topology of Magnetic Insulators with Inversion Symmetry

Ari M. Turner, Yi Zhang, Roger S. K. Mong, Ashvin Vishwanath

Department of Physics, University of California, Berkeley, California 94720, USA

(Dated: January 3, 2012)

We study three dimensional insulators with inversion symmetry, in which other point group symmetries, such as time reversal, are generically absent. We find that certain information about such materials' behavior is determined by just the eigenvalues under inversion symmetry of occupied states at time reversal invariant momenta (TRIM parities). In particular, if the total number of -1 eigenvalues at all TRIMs is *odd* then the material cannot be an insulator. A likely possibility is that it is then a "Weyl" semimetal. If the material *is* an insulator and has vanishing Hall conductivity, then a magnetoelectric response, parameterized by θ, can be defined, and is quantized to $\theta = 0$, π. The value is π if the total number of TRIM parities equal to -1 is *twice an odd number*. This generalizes the rule of Fu and Kane that applies to materials in which time reversal is unbroken. This result may be useful in the search for magnetic insulators with large θ. These two results are obtained as part of a classification of the band topology of inversion symmetric insulators. Such band structures can be classified by two sets of numbers: the TRIM parities and three Chern numbers. The TRIM parities have the physical implications just described, and additionally they constrain the values of the Chern numbers modulo 2. An alternate geometrical derivation of our results is obtained by using the entanglement spectrum of the ground state wave-function.

PACS numbers:

I. INTRODUCTION

Certain electromagnetic phenomena in insulators are insensitive to details about the material. They result from a) topology of the bands (or the indecomposability of the insulator into separate atoms) and b) symmetry. The quantized Hall effect is the most striking example–in a strong magnetic field, a two dimensional gas of electrons becomes insulating (in the sense that there is no thermal conductivity) but has a Hall current when an electric field is applied: $J_H = \sigma_H E$ with $\sigma_H = N\frac{e^2}{h}$ quantized[1]. The same effect can, in principle, occur in a two-dimensional material or film–the lattice does not stop the Hall current, if sufficiently weak, and an applied magnetic field can be simulated by electromagnetic interactions of the electrons and nuclei. The Hall coefficient is usually thought of as being connected to the particular filling fraction of Landau levels, but the more general explanation is that it is related to the topology of the band structure of the electrons. Thus it is unchanged by continuous changes in the crystal lattice.

A real class of materials[2], known as topological insulators, exhibit similar topological phenomena. (Materials that have the actual intrinsic Hall effect have not been found yet.) The materials that have been discovered have time-reversal symmetry. They should have two interesting behaviors–there are "protected" surface states (observed with ARPES, for instance), and there should be a "magnetoelectric response"[3,4] (not yet seen) in which (e.g.) an applied electric field induces a magnetization $M = \theta\frac{e^2}{2\pi h}E$. The magnetoelectric response may be observed only if there is a gap on the surface as well as in the bulk, so the "chiral" surface states must be eliminated by coating the surface with a magnetic material or doping the bulk[5] and getting the Fermi energy into the band gap this produces.

If the material were spontaneously magnetically ordered, one would be able to observe the magnetoelectric effect without treating the surface first. However, materials that break time reversal symmetry in the bulk tend to have a small value of θ, a couple of percent[6]. The origin of the large θ in a topological insulator is related to the time reversal symmetry, surprisingly: symmetries usually force quantities to vanish, but the time-reversal invariance of the insulator keeps θ large. The allowed values of θ are quantized because time-reversal takes $\theta \to -\theta$. This seems to rule out a nonzero θ, but since θ is defined only modulo 2π, 0 and π are both compatible with the symmetry[7].

In this article, we will look at magnetically ordered materials (so that the surface states are gapped) but which have some spatial symmetry group in place of time reversal, in order to keep θ large. One might expect a whole variety of phases as one varies the symmetry group, perhaps displaying effects besides θ, but since there are 230 space groups altogether, we will focus here on a single simple one. This is the symmetry group with just inversion ($\mathbf{r} \to -\mathbf{r}$), a symmetry that is commonly realized in magnetic insulators. For example, all Bravais lattices are inversion symmetric. (Phases of antiferromagnets, with magnetic symmetry groups, can also be classified using a similar approach[9].)

Now, inversion transforms θ the same way as time reversal does, so θ will have two possible values in this case also, 0 and π. Since θ is quantized, there should be a simple rule for determining its value, and in fact we show that the formula of Fu and Kane[10] (originally derived when both time reversal *and* inversion symmetry are present) generalizes to the case with magnetic order, where time reversal is absent.

Rather than focussing solely on the magnetoelectric

effect, we will study a more general question: "Which phenomena in topological insulators can be determined by studying just the symmetry properties of Bloch states at special momenta?" When inversion is the only symmetry, Bloch states at TRIMs (time-reversal invariant momenta) can be classified by their *inversion parities*, which generalize the notion of the sign ± 1 picked up by an orbital wave function of a molecule when it is inverted. In an infinite insulator, inversion parities are defined for the Bloch states at special momenta, those that are left invariant under the inversion $\boldsymbol{\kappa} \to -\boldsymbol{\kappa}$ (the $TRIMs$, which stands for Time-reversal Invariant Momenta). In molecules, parity eigenvalues lead mainly to microscopic effects, such as selection rules for transitions. In bulk, though, phenomena on a large scale can be determined by just these parities, as Fu and Kane's result exemplifies.

When inversion symmetry alone is present, the number of odd states at each of the eight TRIMs can be anything at all (since time reversal is broken, the states do not have to come in pairs). What are the phenomena associated with these parity patterns, which are permitted after the breaking of time reversal symmetry? We find the following phenomena: first, if the total number of odd states *at all TRIMs* is an *odd* integer, then the material is *not insulating*. Second, if the material is insulating and the number of odd states at some *individual* TRIMs is odd, then the material has either *electrostatic polarization* or *bulk quantized Hall conductivity*. Third, if the material is insulating, and the *total* number of odd states is *twice an odd integer* then the material must have a magnetoelectric effect of $\theta = \pi$. It is natural that unpaired odd states at TRIMs can indicate a quantum Hall, since this phenomenon (like the unpaired states) is ruled out by time reversal symmetry.

Of these phenomena, we would like to emphasize the first and the third, about the non-insulating behavior and the magnetoelectric effect. These have some interesting experimental implications. If the product of all the TRIM parities is -1, as for the parity assignment in Fig. 1a, then the material cannot be an insulator (as just mentioned). Such a material is likely to be a "Weyl Semimetal," one of the two classes of semimetal introduced by Ref.[11]. For such parities, the dispersions for the filled and empty bands with the minimum overlap between them have two touching points. These points are called Weyl points. Such materials have thermodynamic and conductivity properties related to their vanishing density of states. Furthermore, they should have interesting quantized responses, corresponding to the "chiral anomalies" of field theory, as pointed out by Volovik[12]. Weyl points cannot occur in a material with both time reversal and inversion symmetry: then energy levels come in Kramers pairs, so the product of the parities is always $+1$.

The formula for θ helps in the search for materials with a large magnetoelectric effect. It shows, as we had hoped, that a magnetic material may have a magneto-electric response but not have protected surface states. Furthermore, the formula for θ suggests that the magnetoelectric effect can occur in materials with essentially no spin-orbit coupling, but which have nonplanar magnetic order. In these materials, nontrivial band topology can be induced by Berry's phases in the hopping amplitudes due to the magnetic order, rather than to the spin orbit coupling (which was required in the time reversal symmetric case).

For an investigation of whether these properties might occur in particular materials, see Ref. 13. This article studies whether the magnetoelectric effect and Weyl metal behavior can be present in magnetically ordered iridates, and finds that the Weyl metal behavior seems to be more likely.

We will begin (Sec. II) with a brief summary of our results, explaining the various conductivity and response properties that are constrained by the inversion symmetry of a band structure.

After this we present the derivation of these results systematically. The goal is to try to find *all* the response properties that are determined by symmetry properties, given inversion symmetry. There are three steps. We begin (Sec. III) by classifying all the phases with inversion symmetry, similar to how the phases with the different Altland and Zirnbauer symmetry groups have been classified before[15,16]. Next (Sec. III B) we identify which of these phases have a chance of having robust dynamical responses. Last (Sec. IV), we determine what the responses are.

The outcome of the classification is that all insulators in three dimensions are parameterized by three Chern numbers and a set of inversion parities. *Chern numbers*, which describe topological properties of the Bloch states as a function of momentum, were already present in the absence of inversion symmetry. The Chern number has three integer components (whereas in two dimensions it is a single integer, in three it is a reciprocal lattice vector). The *inversion parities* can be encapsulated in eight integers describing the number of odd states at each of the TRIMs.

The second step, in Section III B, is a preliminary study to determine which of these phases have the *potential* to have interesting quantized responses. This section organizes the problem–it simplifies a mess of infinitely many phases down to 16. This uses a process of elimination: we first identify the quantum numbers of dull "frozen insulators"; the remaining insulators are the interesting ones.

Section IV contains the last step and the outcome: it determines the quantized responses in the interesting phases and how they are related to the inversion parities. It derives the condition that ensures a material is non-insulating and the criterion for an insulator to be magnetoelectric, as well as some relations between the parities, Hall conductivity and polarization.

This procedure implies that these are the only response properties, even though there are infinitely many differ-

ent ways of assigning inversion parities. Infinitely many of these phases have no response, because they can be realized in ionic crystals, in which each electron is tightly bound to a single atom. After ionic portions of a band structure are separated out, only finitely many phases remain.

At the end, we give an alternative approach based on entanglement. In particular, we will see why the relationships between inversion parities and responses usually depend on the numbers of odd states modulo 2 or 4. The entanglement spectrum of a material is a set of quantities that can be derived from the ground state wave function. It consists of a set of modes that behave like physical surface modes, although they can be determined (at least in principle) without perturbing the system into an excited state, and they can give a signature that a material is in a topological phase[17–19]. Sec. V gives a formula for the number of entanglement modes in an inversion symmetric insulator in terms of the inversion parities. This result is then used to rederive some of the electromagnetic properties in a simple fashion and to understand why all these relations depend on the parities modulo 4.

The present article addresses some questions left open in earlier work in which we participated. Ref.[18] discusses the entanglement spectrum of inversion symmetric insulators, without presenting the exact relation to TRIM parities. The discussion here provides the basis for the investigation in[13] which studied the electronic structure of a specific material (yttrium iridate) using the constraint on the total number of odd states and expressions for θ in terms of the TRIM parities.

The formula derived here for the magnetoelectric effect depends on the inversion parities in the same way as Fu and Kane's formula, but it applies to a wider class of materials, including materials that cannot even be adiabatically connected to any material with time reversal symmetry.

The first prediction–that a material with an odd number of states is metallic–has an interesting corollary that has been noticed before–if time-reversal symmetry is broken, then continuous transitions between $\theta = 0$ and $\theta = \pi$ insulators cannot be found generically[20]. A metallic (or Weyl-metal) phase intervenes except possibly at isolated points.

II. SUMMARY OF RESULTS

Let us first define some conventions about the crystal lattice. We will for simplicity assume that the lattice is cubic (although there is no symmetry beyond inversion) and has a lattice spacing equal to one unit. All quantities will be written with respect to a coordinate system xyz that is aligned with the axes of the crystal. The primitive lattice vectors are $\mathbf{R}_i$ (i.e., the unit vectors along the axes) and the reciprocal lattice vectors are $\mathbf{g}^i$ where $\mathbf{g}^i \cdot \mathbf{R}_j = 2\pi\delta_j^i$. If one wants to apply the results to a non-cubic crystal, it is possible to translate the results

described here to any lattice, by interpreting the expressions in the right coordinate system[21].

To study insulators with inversion symmetry it is useful to look at inversion parities, as in the study of spectra of small molecules. Such parities seem to describe static properties of wave functions, yet in a bulk material, they can determine how electrons move in response to a field. The point of this article is to understand such relationships. The numbers of occupied states with each parity provides integers that can be used to classify the phases (analogous to how "topological integers" are used to understand other types of phases, for example, the quantum Hall conductance in Hall insulators or the Z_2 index for strong topological insulators). The main techinical distinction between solids and molecules is that, in solids, the occupied states can be labelled by momentum. Let these states be given by $\psi_{i\mathbf{k}}(\mathbf{r}) = u_{i\mathbf{k}}(\mathbf{r})e^{i\mathbf{k}\cdot\mathbf{r}}$. States at the "TRIMs" (and only these) can be classified by parity under inversion. The TRIMs are the momenta given by

$$\boldsymbol{\kappa} = \frac{n_1}{2}\mathbf{g}_1 + \frac{n_2}{2}\mathbf{g}_2 + \frac{n_3}{2}\mathbf{g}_3 \qquad (1)$$

where n_1, n_2, n_3 are integers. Such a momentum maps to itself under inversion symmetry modulo the reciprocal lattice, $-\boldsymbol{\kappa} \equiv \boldsymbol{\kappa}$. Hence the wave functions at $\boldsymbol{\kappa}$ must be invariant, and their parities can be defined:

$$\mathcal{I}\psi_{a\boldsymbol{\kappa}}(\mathbf{r}) = \eta_a(\boldsymbol{\kappa})\psi_{a\boldsymbol{\kappa}}(\mathbf{r}) \qquad (2)$$

Appendix A explains how to find these parities using a tight-binding model.

We now introduce a key quantity $n_o(\boldsymbol{\kappa})$ at every TRIM $\boldsymbol{\kappa}$. This is defined as the *number of states with odd parities* at that TRIM. Note, these cannot change without a phase transition (at least in a non-interacting system). Besides these 8 integers, the quantum Hall conductance gives three more invariant integers, since it is quantized: $\mathbf{G}_H = \frac{e^2}{2\pi h}\tilde{\mathbf{G}}_H$ where $\frac{\tilde{\mathbf{G}}_H}{2\pi}$ has integer components (according to the conventions defined above).

For inversion symmetric insulators, the Chern numbers and the n_o-counts of odd states give parameters that can be used to distinguish among phases. Furthermore, these 11 integers, together with the total number of occupied bands n, give a complete description of the set of phases– any two band structures with the same integers can be tuned into one another without a phase transition. This scheme is derived in Sec. III. Appendix B gives an alternative method that is easier to generalize.

Certain physical properties of each phase can be predicted in terms of these integers. We will find all the basic observable quantities that can be expressed in terms of the n_o's.

Total Parity Constraint and Metallic Behavior: The first two relationships between physical properties and inversion parities can be written in terms of *net* parities:

$$\eta_{\boldsymbol{\kappa}} = (-1)^{n_o(\boldsymbol{\kappa})} = \prod_a \eta_a(\boldsymbol{\kappa}). \qquad (3)$$
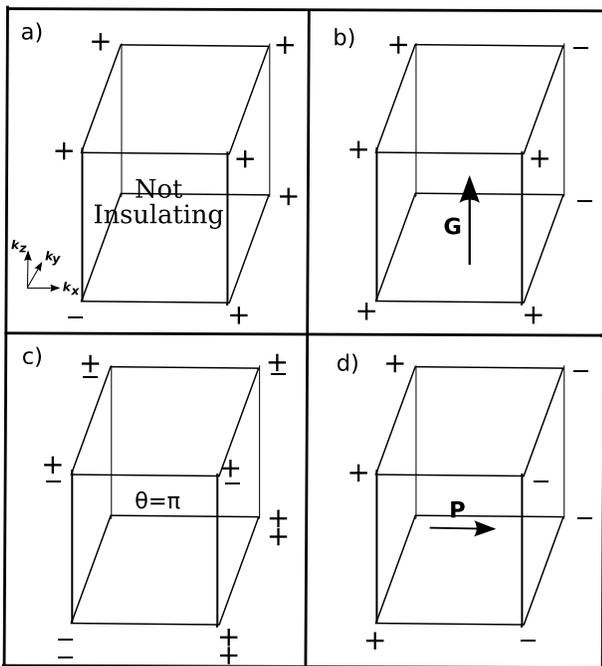
FIG. 1: Determining properties of systems using parities. The boxes represent an eighth of the Brillouin Zone; the TRIMs are at the corners. The signs represent the parities of the occupied states at the TRIMs. In (a) the parity constraint of even number of odd parity states is violated, hence it cannot be an insulator. In (b) the parities require a nonvanishing Hall conductance, with odd Chern number in the $k_x k_y$ planes. (c) Quantized magnetoelectric response $\theta = \pi$ determined from number of odd parity states being 2 (mod 4). (d) A parity configuration corresponding to a frozen polarization.

For any insulator, one can show:

$$\prod_{\boldsymbol{\kappa}} \eta_{\boldsymbol{\kappa}} = 1. \tag{4}$$

That is, the total number of filled odd parity states must be even. This is shown in Sec. IV A.

The contrapositive of this statement is the most interesting form of it: if, for some band structure, $\prod_{\boldsymbol{\kappa}} \eta_{\boldsymbol{\kappa}} = -1$, then the system must be gapless. For example, if a system has the parities in Fig. 1a, it must be metallic, because there are an odd number of odd occupied states. The gap must close at some momentum $\mathbf{k}$ in the Brillouin zone.

Materials with $\prod_{\boldsymbol{\kappa}} \eta_{\boldsymbol{\kappa}} = -1$ should be interesting. They will have Weyl points, three dimensional points where the valence and conduction bands meet with a dispersion shaped like a cone. Under certain circumstances, the Fermi energy is expected to pass right through the cone points, so that the material is a semimetal with a density of states that is equal to zero.

Note that the right hand side in Eq. (4) differs from the index $(-1)^{\delta_0}$ used by Fu and Kane–their index is only the product of the parities of "half" the occupied states; since they focused on systems with both time reversal and inversion symmetry, the states always come in pairs due to Kramers's theorem. The product in Eq. (4) is automatically equal to 1 when these symmetries are present, so it did not come up in that context. The result in Eq. (6), below, generalizes the strong index.

Quantum Hall Effect. The net parities also determine the quantum Hall integers modulo 2. The z-component of $\tilde{\mathbf{G}}_{\mathbf{H}}$, for example, satisfies

$$e^{\frac{i}{2}\tilde{G}_{Hz}} = \prod_{\substack{\boldsymbol{\kappa}; \\ \boldsymbol{\kappa} \cdot \mathbf{R}_z = 0}} \eta_{\boldsymbol{\kappa}} \tag{5}$$

That is, whether the Hall conductivity along the z-direction is an even or odd multiple of 2π can be determined by multiplying the η's around either of the squares parallel to the xy-plane. This result is derived in Sec. IV B.

If a system has the parities shown in Fig. 1b, the Hall conductivity cannot vanish. The component along the z-direction, G_{Hz}, must be an odd multiple of $\frac{e^2}{hc}$ (per layer of the crystal).

Eqs. (4),(5) also have a formal interpretation: they are constraints between the invariants of insulating phases. The 11 integers $\tilde{\mathbf{G}}_{\mathbf{H}}$ and $n_o(\boldsymbol{\kappa})$ are not completely independent of one another, but have to satisfy these four relationships between their parities. Moreover, these are the only constraints–if the relationships are satisfied, the invariants can be realized in principle in some band structure.

Magnetoelectric Effect We also find the magnetoelectric effect. This effect is related to the magnetoelectric polarizability α_j^i. An applied magnetic field induces a polarization, $P^i = \alpha_j^i B^j$. In the absence of the quantum Hall effect, α_j^i is well-defined. (Otherwise the polarization can be neutralized by a flow of charge in the surface states associated with the Hall effect.) The polarizability α_j^i is odd under inversion: Under inversion symmetry, $\mathbf{P}$ changes sign, while $\mathbf{B}$ does not.

If the crystal is inversion symmetric, it seems that α must vanish. However, α is ambiguous. An isotropic portion ($\frac{e^2}{h} \delta_{ij} \times$ integer) is indeterminate because it can be mimicked by an integer quantum Hall coating on the surface. Thus α_j^i can be inversion symmetric if it is isotropic and has a quantized value: $\frac{e^2}{2\pi h}\theta\delta_j^i$, where θ is a multiple of π.

Earlier work has considered θ for the case of materials with *time reversal* symmetry. In that context, the magnetoelectric effect (i.e., $\theta = \pi$) and a nonzero strong index are two aspects of the same phenomenon[3,4]. If the system also has inversion symmetry, the criterion under which these phenomena occur was found by Fu and Kane[10]. We find that essentially the same formula can be used to determine when $\theta = \pi$ even when the time reversal symmetry is not present. This formula depends

on the n_o parameters, and not just the η_κ's:

$$\frac{\theta}{\pi} \equiv \frac{1}{2} \sum_\kappa n_o(\kappa) \quad (\text{mod } 2). \tag{6}$$

According to Eq. (4), this is always an integer. This expression is proved in Sec. IV C.

This result is somewhat more general than the results for materials with time reversal as well as inversion symmetry, because the details of the band structure can be quite different in the presence of magnetism: when time reversal is broken, there may be an odd number of occupied states at some of the TRIMs. Such band structures cannot even be adiabatically connected to the band structure of a material with time reversal symmetry because of Kramers's theorem, yet the magnetoelectric effect is still determined by Eq. (6).

One such band structure is illustrated in Fig. 1c; it is not adiabatically connected to any insulator with time reversal symmetry because of the unpaired odd states at the TRIMs. Although the number of odd states at each individual TRIM in Fig. 1c is either even or odd, the total number of odd states is even (in accord with Eq. (4)) and is twice an odd number: hence $\theta = \pi$.

One may concoct examples of Hamiltonians on a cubic lattice with such patterns of parities. One constructs a hopping model where the local orbitals are labelled as being even-type orbitals $(s, d, \dots)$ or odd-type orbitals $(p, f, \dots)$. Electrons can hop between these orbitals. The hopping matrix elements can be chosen almost arbitrarily except that they must respect inversion symmetry, which constrains the relative signs of hopping in two opposite directions. If orbital a is centered around a point of inversion symmetry, $t_{a \to b} = \pm t_{a \to b'}$ where the orbitals b and b' are corresponding orbitals on sites displaced from orbital a in opposite directions. The sign depends on whether a and b have the same or opposite parities. App. A describes such a Hamiltonian (with third-neighbor hopping) in more detail, with the parities illustrated in Fig. 2a.

Frozen Polarization. Finally, let us complete the discussion of physical properties that are constrained by the "net parities" $\eta_\kappa = \pm 1$. Eq. (5) shows that they determine the Chern numbers modulo 2. This accounts for three of the eight independent bits of information contained in the parities. Note that any pattern of parities satisfying the constraint Eq. (4) can be factored into 7 basis patterns:

$$\eta(\kappa) = \pm(-1)^{\frac{1}{\pi^2}\tilde{g}_x \kappa_y \kappa_z}(-1)^{\frac{1}{\pi^2}\tilde{g}_y \kappa_x \kappa_z}(-1)^{\frac{1}{\pi^2}\tilde{g}_z \kappa_x \kappa_y}(-1)^{\frac{2}{\pi}\tilde{\mathbf{P}}_e \cdot \kappa}. \tag{7}$$

This factors into seven parts: the three factors depending on $\tilde{g}_i$, the three depending on $\tilde{\mathbf{P}}_e$ and the overall sign in front. (Note that the components of $\tilde{\mathbf{P}}_e$ are half-integers while those of $\tilde{\mathbf{g}}$ are integers. The factors of π are included to make the exponents into integers.) The pattern corresponding to $\tilde{g}_z = 1$ (and all other $\tilde{\mathbf{g}}$ and $\tilde{\mathbf{P}}_e$ variables set to 0) is just the same one shown in Fig.

1b. Hence $\tilde{\mathbf{g}}$ is just the Hall conductivity modulo 2. The patterns of η_κ on the vertices of the cube corresponding to some $\tilde{\mathbf{P}}_e$ (with $\tilde{\mathbf{g}}$ set to zero) vary as a plane wave. The wave-number, $\tilde{\mathbf{P}}_e$ turns out to determine the intrinsic polarization.

Intrinsic electrical polarization is a phenomenon found in ferroelectrics. When analyzed carefully[14], one finds that it is ambiguous like θ: the total polarization can be altered by charges on the surface, but an intrinsic part of it is determined by the bulk properties. The intrinsic portion is determined modulo a lattice vector times e. Inversion symmetry constrains the components to be integers or half-integers times e. Hence the polarization is determined by three bits, which are revealed in (7). $\mathbf{P}_e$ actually describes only the polarization of the electrons relative to the Bravais lattice; one also needs to include the compensating charges of the nuclei:

$$\mathbf{P} = e\tilde{\mathbf{P}}_e - \sum_i Z_i e \mathbf{r}_{Ni}, \tag{8}$$

where $\mathbf{r}_{Ni}$ is the position vector of the ith nucleus, with charge $-Z_i e$. This result is derived in Sec. IV B.

Consider the polarization of the crystal with the band structure illustrated in Fig. 1d; it is $\frac{e}{2}\mathbf{R}_1$ if the nuclei are all on the sites of the Bravais lattice. This quantity is called "intrinsic polarization," but it does not actually appear as a polarization all the time. When it is nonzero, it *could* lead to a ferroelectric moment, so that the crystal would have a surface charge of $\frac{1}{2}e$ per unit cell and a large electric field. The alternative possibilities are more likely: the translational symmetry of the surface may be spontaneously broken or the surface may be metallic (see Ref. 22, summarized in appendix G).

Other effects? There are many combinations of parities an insulator could have and yet not display any of the phenomena described above. Such insulators cannot be characterized in any other macroscopic way either. They belong to distinct phases (there are gapless regions between them in a phase diagram), but these phases all behave in the same way. For example, if there are 4 odd states at $\kappa = 0$, and 4 even states at all other TRIMs, then Eqs. (5), (6), and (7) give trivial Hall conductivity, θ, and polarization. This phase is definitely a distinct phase, separated by a phase transition, from the one where all states are even, so it may seem likely that some other property would distinguish the two phases. However, Sec. III B shows that no response property distinguishes this phase (or any insulating phase θ, the Hall coefficients, and the polarization vanish).

Parity constraints in general dimensions. The results in higher dimensions have a surprising feature: as the number of dimensions increases the sum of the n_o's must be divisible by larger and larger powers of 2 if the material is to be insulating.

Specifically, in $2s$ dimensions, the sum of the n_o's is a multiple of 2^{s-1}. This multiple is related to the $2s$-dimensional Chern number $\tilde{G}_{2s}$ (defined as a multiple of

$$\frac{1}{2^{s-1}} \sum_{\text{TRIM } \boldsymbol{\kappa}} n_o(\boldsymbol{\kappa}) \equiv \frac{\tilde{G}_{2s}}{2\pi} \pmod 2; \qquad (9)$$

the quantum Hall conductance is the 2-dimensional special case.

In $2s+1$-dimensions, the sum of the n_o's is a multiple of 2^s and is related to the Chern-Simons integral

$$\frac{\theta_{2s+1}}{\pi} = \frac{1}{2^s} \sum_{\boldsymbol{\kappa}} n_o(\boldsymbol{\kappa}) \pmod 2. \qquad (10)$$

where the polarization and magnetoelectric effect are the one- and three-dimensional versions.

Note that insulators with inversion symmetry are quite different from ones without any assumed symmetry: There is an insulator in $2s$ dimensions with a Chern number $\tilde{G}_{2s}$ equal to 1 which has just s filled bands[23]. This insulator is not inversion symmetric, though. The simplest inversion symmetric insulator with the identical Chern number has a minimum of 2^s bands, exponentially more bands than are necesary without symmetry.

The Entanglement Spectrum. The entanglement spectrum (a concept used to study quantum fluctuations[24]) produces an alternative explanation for these results. Each of the phenomena is connected to a certain type of "entanglement surface state." These states may be counted using inversion symmetry. An insulator with inversion symmetry has a particle-hole symmetry $\mathcal{I}_e$ in its entanglement spectrum $\epsilon_a(\mathbf{k})$ when it is cut on a plane through a center of inversion. This makes it very easy to determine qualitative properties of the Fermi arcs of the entanglement spectrum–it is possible to count (without topological arguments) the number of zero modes in the entanglement spectrum at the TRIMs $\boldsymbol{\kappa}_\perp$ along the surface. Let $\Delta N_e(\boldsymbol{\kappa}_\perp) = \text{tr}_{\epsilon=0}\mathcal{I}_e$; that is $\Delta N_e(\boldsymbol{\kappa}_\perp)$ is the number of even modes minus the number of odd modes with zero entanglement-energy at $\boldsymbol{\kappa}_\perp$.

The $\Delta N_e(\boldsymbol{\kappa})$ parameters can be expressed in terms of parities of the bulk states through $n_o(\boldsymbol{\kappa})$. (The parities of the bulk states are to be defined using an inversion center on the plane of the entanglement cut.) The quantity that appears is $\Delta N(\boldsymbol{\kappa}) = \text{tr}_{E<0}\mathcal{I}$, or $n - 2n_o(\boldsymbol{\kappa})$:

$$\Delta N_e(\boldsymbol{\kappa}_\perp) = \frac{1}{2}(\Delta N(\boldsymbol{\kappa}_1) + \Delta N(\boldsymbol{\kappa}_2)), \qquad (11)$$

where $\boldsymbol{\kappa}_1$ and $\boldsymbol{\kappa}_2$ are the two TRIMs that project to $\boldsymbol{\kappa}_\perp$. In words: the difference between the number of even and odd states on the entanglement "Fermi surface" at a TRIM is half the difference between the even and odd states in the bulk, at the corresponding TRIMs.

To illustrate an actual entanglement spectrum, we constructed a Hamiltonian with a cubic unit cell whose inversion parities suggest that $\theta = \pi$ and $\tilde{G}_{Hi} \equiv 0 \pmod 2$. The parities and the spectrum are shown in Fig. 2. (The Hamiltonian is described in Appendix A.) The entanglement spectrum was calculated for a cut along the xy-plane. As expected, there is a Dirac point at $(0,0)$,
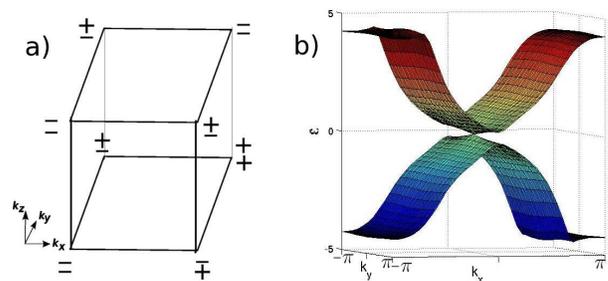

FIG. 2: Entanglement spectrum of a hopping Hamiltonian. a) The parities at the TRIMs. b) The entanglement modes on a cut parallel to the xy-plane. Note that there are two zero-modes at the TRIM $(0,0)$ and none at the other TRIMs, as expected from the parities.

although there are no physical surface states. The entanglement states reflect the nonzero θ, though physical states do not.

From the relation between the entanglement spectrum and the parities, one can give alternative derivations of the connections between electromagnetic properties and inversion parities. This formula also leads to a simple alternative derivation of Fu and Kane's formula for the indices of topological insulators. These indices count the *physical* surface states. The entanglement states are easy to count with the help of symmetry, and they can be continuously deformed into the physical spectrum.

III. CLASSIFYING INVERSION SYMMETRIC INSULATORS

This section will show why the inversion parities and the Chern numbers give the full classification of noninteracting insulators with inversion symmetry. This result follows from the classification of Hamiltonians without any symmetry, because the space of inversion symmetric Hamiltonians and the space of all Hamiltonians are related. The Hamiltonians without symmetry are already classified by Chern numbers for each two-dimensional cross-section of the Brillouin zone. The only additional parameters that appear when the Hamiltonians have to be inversion symmetric come from the classification of "zero-dimensional insulators" associated with the TRIMs. Like finite molecules, these states can be classified by inversion parities.

Consider the Hamiltonian $H(\mathbf{k})$ for the wavefunctions $\psi_{n\mathbf{k}}$. This Hamiltonian can be taken to be an $N \times N$ matrix by using a tight-binding model with N bands (n of which are filled). Since this Hamiltonian is inversion symmetric,

$$I_0 H(\mathbf{k}) I_0 = H(-\mathbf{k}) \qquad (12)$$

where I_0 is the matrix describing how the orbitals within the unit cell transform under inversion[25].

For non-interacting insulators, a phase transition occurs when the gap closes and states cross the Fermi energy, $\mu = 0$, say. Let us determine when two Hamiltonians are in the same phase–i.e., can be connected without a phase transition. Topologically speaking, we consider matrix fields $H(\mathbf{k})$ and define an equivalence relationship:

$$H(\mathbf{k}) \sim H'(\mathbf{k}) \text{ if } H(\mathbf{k}) \text{ can be deformed to } H'(\mathbf{k})$$
$$\text{without any eigenvalues vanishing and}$$
$$\text{while maintaining inversion symmetry.} \quad (13)$$

The only points in the Brillouin zones where the inversion symmetry constrains the Hamiltonian are the TRIMs, $\boldsymbol{\kappa}$. Each of these points can be interpreted as a zero-dimensional system, with a Hamiltonian $H(\boldsymbol{\kappa})$ that is invariant under I_0, since Eq. (12) implies $I_0 H(\boldsymbol{\kappa}) I_0 = H(\boldsymbol{\kappa})$. Let $n_o(\boldsymbol{\kappa})$ be the number of eigenvalues at negative energy which are odd under I_0. As the Hamiltonian evolves, the states at this TRIM can mix together, but even states can mix only with even states and odd ones can mix only with odd ones, so the value of $n_o(\boldsymbol{\kappa})$ cannot change.

The second set of parameters characterizing the Hamiltonian are the Chern numbers which are topological winding numbers that also turn out to describe the Hall conductivity[26,27]. Because they are integers, they are also invariant.

We will now show that these integers give a complete classification of Hamiltonians with inversion symmetry. That is, if $H(\mathbf{k})$ and $H'(\mathbf{k})$ are two Hamiltonians both with n occupied states, N states total, N_o of which are odd, then they can be deformed into one another while preserving inversion symmetry (i.e., $H(\mathbf{k}) \equiv H'(\mathbf{k})$) if

$$n_o(\boldsymbol{\kappa}) = n'_o(\boldsymbol{\kappa}) \text{ (for all TRIMs } \boldsymbol{\kappa})$$
$$\tilde{\mathbf{G}}_H = \tilde{\mathbf{G}}'_H, \quad (14)$$

at least if $N - n, n \geq 2$.

We do not usually consider the integers N and N_o to be important invariants–their values can be changed by adding even or odd orbitals with a very high energy. In continuous space, there are infinitely many available orbitals.

The assumption $N-n, n \geq 2$ is included because, when there are too few bands, there are some Hamiltonians that cannot be deformed into one another just because there are not enough degrees of freedom.[28][29] Our classification theorem does not capture these distinctions, but the distinctions are not related to any generic properties. If one adds sufficiently many trivial occupied and unoccupied bands to an insulator, any two insulators with the same invariants can be deformed into one another.

A. Proof that n_o and G_H Classify Inversion Symmetric Insulators

Here we present the essential ideas of the proof of the classification of insulators. App. B gives a more systematic way of deriving the classification, including higher dimensions.

The result can be derived by relating a Hamiltonian in d dimensions to one in a smaller number of dimensions, starting with $d = 3$. Let us take d to be arbitrary at first, so that we can describe the general procedure for reducing the number of dimensions. Let $\mathcal{H}_d$ be the space of general Hamiltonians in d dimensions, while $\mathcal{I}_d$ is the subspace of Hamiltonians that have inversion symmetry. A generic Hamiltonian in $\mathcal{H}_d$ can be regarded as a closed loop in $\mathcal{H}_{d-1}$: Fixing the dth component of $\mathbf{k}$ to have an arbitrary value k_d results in a $d-1$-dimensional Hamiltonian H_{k_d}, $H_{k_d}(k_1, k_2, \ldots, k_{d-1}) \equiv H(k_1, k_2, \ldots, k_d)$. As k_d varies, H_{k_d} traces out a closed loop in $\mathcal{H}_{d-1}$ because the Brillouin zone is periodic.

A Hamiltonian in $\mathcal{I}_d$ has an alternative representation, as just an arc in $\mathcal{H}_{d-1}$, half of the loop just described (from $k_d = 0$ to π). The rest of the loop is determined by the inversion symmetry. The end-points of this arc have to be on $\mathcal{I}_{d-1}$ because the inversion takes the $k_d = 0, \pi$ cross-sections to themselves.

Thus, classifying inversion symmetric Hamiltonians is equivalent to the problem of classifying which arcs can be deformed into one another, as illustrated in Fig. 3. That is, consider arcs γ_1, γ_2 in $\mathcal{H}_{d-1}$ connecting two points in the subspace $\mathcal{I}_{d-1}$. What conditions ensure that it is possible to move arc γ_1 to arc γ_2? This deformation is possible if we can first slide the end-points of γ_1 within $\mathcal{I}_{d-1}$ onto the end-points of γ_2 and then smoothly deform the curves connecting them. That is, two arcs are equivalent if their end-points are in the same component of $\mathcal{I}_{d-1}$ (like γ_1 and γ_2 in the figure) but do not have any hole in between them.

We can thus classify d-dimensional Hamiltonians by solving two problems: describing the different components of $\mathcal{I}_{d-1}$, and classifying the arcs connecting a pair of points in $\mathcal{H}_{d-1}$ up to homotopy.

Let us now consider $d = 3$. The first step (classifying the end-points) is analogous to the problem we are trying to solve, just in one dimension less. (The connected components of $\mathcal{I}_2$ are just the different classes of 2-dimensional inversion-symmetric Hamiltonians as defined in Eq. (13).) Let us suppose we know how to deform the two arcs γ_1, γ_2 so that their end-points are the same under the assumptions of Eq. (14).

We now have to slide the *interior* of arc 1 onto arc 2. Classifying arcs with fixed end-points in a given space is closely related to classifying closed loops. For example, consider the complex plane with a hole at the origin. Paths connecting a fixed pair of points are classified by $\int d\theta$ (where θ is the polar angle) just as closed loops are: the possible values of the integrals are separated by multiples of 2π (corresponding to the number of times the path encircles the origin) offset by the angle between the points. The *loops* in $\mathcal{H}_2$ can be classified by two winding numbers $\oint d\alpha(k_z)$ and $\oint d\beta(k_z)$, where α and β are angular variables around holes in $\mathcal{H}_2$. This is a restatement of the well-known fact that the Hamiltonians
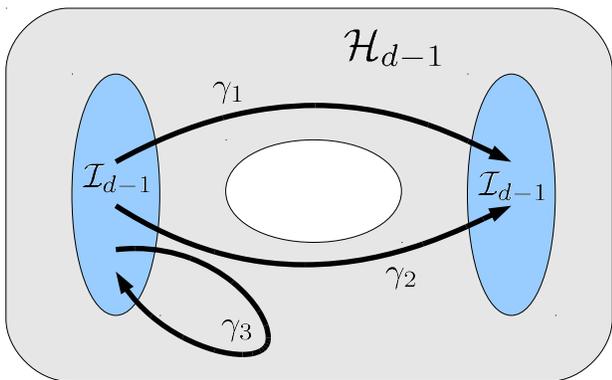
FIG. 3: Representation of d-dimensional Hamiltonians by arcs and loops in the space of $d-1$-dimensional Hamiltonians. The grey region represents $\mathcal{H}_{d-1}$: each point corresponds to a generic d-1-dimensional Hamiltonian. The two ellipses on the side represent the components of $\mathcal{I}_{d-1}$, the Hamiltonians with inversion symmetry. Inversion-symmetric d-dimensional Hamiltonians (three of which are shown) are represented by arcs connecting points in $\mathcal{I}_{d-1}$. Two of these Hamiltonians are equivalent if the end-points are in the same component of $\mathcal{I}_{d-1}$ and have the same winding numbers around holes in the space (represented by the white ellipse). For example, γ_2 and γ_3 are not equivalent because their final end-points are in different components; γ_1 and γ_2 are not equivalent because $\gamma_1\gamma_2^{-1}$ winds around the hole.

in $\mathcal{H}_3$ are classified by their Chern numbers. A loop corresponds to a three-dimensional Hamiltonian without any special symmetry. The two winding numbers equal the $\tilde{G}_{Hx}$ and $\tilde{G}_{Hy}$ Chern numbers of this Hamiltonian. The remaining Chern number is not important because it is determined by the base-point of the loop.

Now it follows, by analogy with the example of arcs in the complex plane, that an *arc* connecting two fixed points in the space $\mathcal{H}_2$ can be classified by the change in α and β. The inversion symmetric Hamiltonians can therefore be classified by $\Delta\alpha = \int_0^\pi d\alpha(k_z)$ and $\Delta\beta = \int_0^\pi d\beta(k_z)$.

The Chern numbers $\tilde{G}_{Hx}$ and $\tilde{G}_{Hy}$ of the full Hamiltonian are given by $\oint_{-\pi}^\pi d\alpha(k_z), \oint_{-\pi}^\pi d\beta(k_z)$; hence the "winding numbers" of the open arcs are half as big as the Chern numbers, (by inversion symmetry). So if the Chern numbers of the Hamiltonians are equal, then the arcs have the same values of $\Delta\alpha$ and $\Delta\beta$ and so they are equivalent.

We now have to return to the problem of showing that the end-points can be slid to one another under the assumptions. This is the same as classifying inversion symmetric Hamiltonians in *two* dimensions. This problem may be solved by studying arcs and loops in $\mathcal{H}_1$.reducing it by one more dimension. For two Hamiltonians in $k_x - k_y$ space to be equivalent, the single winding number, $\tilde{G}_{Hz}$, must be the same, and the one-dimensional

boundary Hamiltonians must be equivalent.

Now we must classify inversion-symmetric Hamiltonians in *one* dimension, i.e., arcs in $\mathcal{H}_0$. There are no winding numbers in $\mathcal{H}_0$, so the problem reduces directly to classifying the zero-dimensional end-points.

Two *zero*-dimensional Hamiltonians (i.e., matrices!) are clearly equivalent if the numbers of even and odd occupied states are the same–just shift the energy eigenvalues so that the two Hamiltonians match. Hence the last condition is that the eight integers $n_o(\boldsymbol{\kappa})$ and the total number of occupied states n must match. The number of even and odd unoccupied states above the Fermi energy must also be the same, but as mentioned above, there are an infinite number of these in continuous space. The original Hamiltonian has bifurcated into eight zero-dimensional Hamiltonians since each step of passing from arcs to end-points doubles the number of Hamiltonians.

Hence, three dimensional Hamiltonians are classified by $\tilde{G}_{Hx}, \tilde{G}_{Hy}$ and $\tilde{G}_{Hz}$ together with the parities at the TRIMs.

B. A Coarser Classification: Grouping Phases with Identical Responses

We would now like to look for physical interpretations of the parities that classify the phases. One often uses parity symmetry to prove that a quantity vanishes, as in selection rules for certain types of transitions in a molecule. We will find that, in bulk systems, some sets of inversion parities imply the *non*-vanishing of a physical quantity. We would like to determine all such relationships.

We will search for sets of parities $\mathbf{n_o}$ that ensure that a material has nontrivial responses by considering the opposite problem. That is, we will first find all the dull insulators, ones in which the electrons cannot move and therefore do not have any response: we call them frozen insulators. Then we will know by a process of elimination which materials have a chance of having an interesting response. We will find that many of the combinations of n_o's can occur in frozen insulators. Hence, even though the n_o quantum describe infinitely many phases, only finitely many of them have distinctive behavior. In the next section, we will determine the behavior for each of the phases with distinct properties.

To picture the different types of insulator, represent the n_o quantum numbers geometrically, as a vector in an eight dimensional cubic lattice. Let us understand the crystal structure of this imaginary crystal. The n_o-vectors for "frozen states" form a sublattice. One may imagine that there are two "elements" A and B making up the compound, with the element A residing at the frozen insulator sublattice, and the other element residing at the remaining sites. The vectors of frozen states form a sublattice because the sum of two frozen vectors is also frozen: combining the orbitals of two materials together in the same volume of space (without any in-
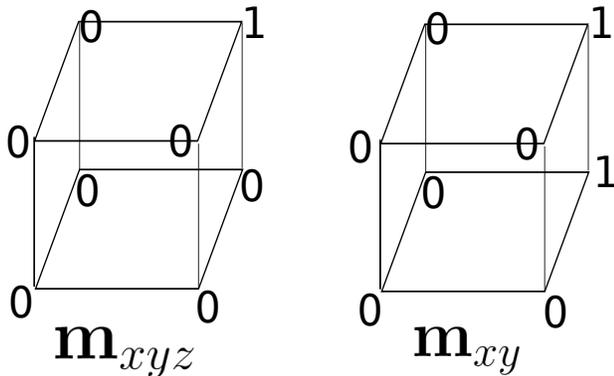
FIG. 4: Representative examples of $\mathbf{n_o}$ vectors for non-frozen band structures. The whole range of quantized behavior that can be found in insulators with inversion symmetry can be found in just these two examples or small linear combinations of them (and the two rotations of $\mathbf{m_{xy}}$), because they form a basis for the unit cell of the 8-dimensional lattice of frozen and non-frozen $\mathbf{n}_o$ vectors.

teractions between them) corresponds to adding their n_o vectors.

The frozen sublattice can then be characterized by some conditions similar to the description of a face-centered cubic lattice. (The face-centered cubic lattice, e.g., sodium ions in table salt, NaCl, is the sublattice of a cubic lattice consisting of the points whose coordinates sum to an even number.) For the crystal of $\mathbf{n_o}$ vectors, the frozen sub-lattice is described as follows. Define $w_{xyz} = \sum_{\boldsymbol{\kappa}} n_o(\boldsymbol{\kappa}) \bmod 4$ and $u_z = \sum_{\boldsymbol{\kappa} \perp \mathbf{R}_z} n_o(\boldsymbol{\kappa}) \bmod 2$, and similarly for u_x, u_y. Then a frozen site is one where these remainders are all zero. (See App. C.)

For example, consider an insulator with these parities: 4 odd states at $\boldsymbol{\kappa} = 0$ and all other states even. It satisfies the conditions $w_{xyz} = u_x = u_y = u_z = 0$. Hence it is in a frozen phase.

Since there are four possible values for w_{xyz} modulo 4 and 2^3 possible values for the u's, this crystal has the chemical formula AB_{31}, that is, the unit cell contains 32 lattice points; one is frozen, and the other 31 can be represented in terms of four vectors (see Fig. 4):

$$\boldsymbol{n}_o = u_{xy}\boldsymbol{m}_{xy} + u_{xz}\boldsymbol{m}_{xz} + u_{yz}\boldsymbol{m}_{yz} + w_{xyz}\boldsymbol{m}_{xyz} \quad (15)$$

where the u's are each 0 or 1 and w_{xyz} is $0, 1, 2$ or 3.

Compounds occupying equivalent positions in the $\mathbf{n_o}$ crystal (and with equal Chern numbers) have equivalent quantized response properties[30] as they differ by the addition of a frozen state. In the following sections, we will determine the properties of each of the different types of compound in the unit cell. Since the u's and w_{xyz} distinguish among the 32 sites in a unit cell, it will be these parameters that determine all the quantized response properties. (Note that materials corresponding to equivalent sites in this classifying crystal could have different *static* properties. Likely the only property of this type is that

frozen insulators can have intrinsic electric polarization. Since polarization is defined modulo one-half of a Bravais lattice vector, there are still only a few combinations of the n_o-integers that have interpretations.)

The key step in this reasoning is to identify the frozen crystals and the corresponding n_o vectors. Consider an ionic or frozen insulator with positive nuclei on the Bravais lattice and electrons fixed on certain sites, and with all hopping amplitudes equal to zero. The simplest example that is inversion symmetric involves a single electron per unit cell located at half of a Bravais lattice vector $\mathbf{d} = \frac{\mathbf{R}}{2}$ and its translates. When there are two electrons per unit cell, there is more freedom: they may be located at any point together with its inversion image. From these two cases all other insulators may be constructed.

The parities of the former insulator depend on $\boldsymbol{\kappa}$, and are found by transforming from the localized basis labelled by $\mathbf{R}$ to plane wave states labelled by $\mathbf{k}$, $|\mathbf{d}\rangle_\mathbf{k} = \sum_\mathbf{R} e^{i\mathbf{k}\cdot(\mathbf{R}+\mathbf{d})}|\mathbf{R}+\mathbf{d}\rangle$. Suppose that the orbital occupied by the electron is odd (for example). Then at a TRIM, the inversion eigenvalue is given by

$$\mathcal{I}|\boldsymbol{\kappa}\rangle_\mathbf{d} = -e^{2i\mathbf{d}\cdot\boldsymbol{\kappa}}|\boldsymbol{\kappa}\rangle_\mathbf{d}, \quad (16)$$

hence $n_o(\boldsymbol{\kappa})$ is one for each $\boldsymbol{\kappa}$ such that $\frac{2\mathbf{d}\cdot\boldsymbol{\kappa}}{\pi}$ is even. These eight vectors, which we call $\mathbf{f_d}$, generate the lattice A of frozen insulators within the crystal of n_o vectors that we are using to classify phases. (The additional n_o's that come from frozen insulators with two electrons per unit cell just reproduce $\mathbf{f_{d=0}}$. They have one odd and one even state at each TRIM.) The appendix shows how to determine the unit cell starting from these primitive vectors.

As an example of a state that can be decomposed into frozen insulators, consider a Hamiltonian H with four odd states at $\boldsymbol{\kappa} = 0$ (and no where else). Its $\mathbf{n_o}$ vector may be expressed $\sum_{\mathbf{d}\neq\mathbf{0}} \mathbf{f_d} - 3\mathbf{f_0}$: it is formally a superposition of the eight basic frozen insulators. Because of the minus sign, this argument is not quite correct, and there is no actual frozen insulator with the same parities as H. Nevertheless, the conclusion is still correct–H does not have any special response properties. If one combines H with 3 copies of the $\mathbf{d} = 0$ frozen insulator, one gets a material that *is* in the same phase as a frozen insulator. Therefore H has no special response properties, since the extra electrons added to it cannot change anything.

To see in general that two materials (H_1 and H_2) with the same Chern numbers whose n_o vectors differ by a vector in the frozen lattice have the same response whether the vector has negative or positive coefficients, write $\mathbf{n_{o1}} - \mathbf{n_{o2}} = \sum_\mathbf{p} n_\mathbf{p}\mathbf{f_p}$ and define $\mathbf{f_+}$ to be the sum of just the terms in this sum with positive coefficients, and define $\mathbf{f_-}$ similarly as the sum of the terms with negative coefficients. Then $\mathbf{f_\pm}$ both are realized for ionic crystals. Furthermore, $\mathbf{n_{o1}} + \mathbf{f_-} = \mathbf{n_{o2}} + \mathbf{f_+}$, so the materials obtained by combining the ionic crystals $\mathbf{f_-}$ and $\mathbf{f_+}$ with H_1 and H_2 respectively belong to the same phase. Hence these materials and H_1 and H_2 all have the same quantized response properties.

IV. PHYSICAL PROPERTIES AND THE PARITIES

Now we will find the properties for all the sites in the unit cell of the crystal of n_o vectors. We will study these sites in three stages: the next section shows that sixteen of the sites can occur only in non-insulators; the next one shows that 14 of the remaining ones have a nonzero Hall conductivity, and the last shows that the two remaining insulators can be distinguished by whether they have a magnetoelectric susceptibility or not.

A. Constraint on Parities in Gapped Materials

We will start by showing that if $\sum_{\boldsymbol{\kappa}} n_o(\boldsymbol{\kappa})$ is odd for a certain band structure, then this band structure is not an insulator (Eq. (4)). This determines the basic behavior of a crystal with the $\mathbf{n_o}$ vector $\mathbf{m_{xyz}}$ (see Fig. 4a), and more generally, any state with $w_{xyz} \equiv 1, 3$ (see Eq. (15), since $\sum_{\boldsymbol{\kappa}} n_o(\boldsymbol{\kappa}) \equiv w_{xyz} \pmod 4$

There are two ways to see that $\sum_{\boldsymbol{\kappa}} n_o(\boldsymbol{\kappa})$ must be even in an insulator. For the first one, let us understand a more general question. Consider a Hamiltonian (not necessarily a gapped one) that is being altered. What happens when the parities of the occupied states at the TRIMs change? These parities can change if an even state at the TRIM below the Fermi energy and an odd state above the Fermi energy (or vice versa) pass through one another. Appendix D shows that, each time $n_o(\boldsymbol{\kappa})$ changes by 1 by means of such an interchange, a pair of Weyl points that are inversion images of each other appears or disappears. Weyl points are points in the Brillouin zone when the conduction and valence bands touch, hence when they are present, the material is not an insulator. Therefore, if the insulator starts out as a frozen insulator with all $n_o(\boldsymbol{\kappa}) = 0$, then the first change of $n_o(\boldsymbol{\kappa})$ makes the material non-insulating.

Furthermore, the material cannot become insulating again through a gapping out of the Weyl points, unless more n_o's change. A Weyl point is stable in isolation because it has a "chirality" ± 1 and the total chirality of Weyl points is conserved (see App. D). (In fact, Weyl points are Berry-flux monopoles in momentum space, so they have a conserved charge[31].) A pair of inversion-symmetric Weyl points can either annihilate with a second pair or with one another. The latter cannot occur when the parities at the TRIMs are fixed, because by symmetry they would have to meet one another at a TRIM. Annihilating there would cause a change in the parities at it.

Now start from a trivial (i.e., a frozen) Hamiltonian, with all electrons glued to the Bravais lattice; in this Hamiltonian, all the states at TRIMS are even. After an odd number of changes of $n_o(\boldsymbol{\kappa})$, there are an odd number of pairs of Weyl points, so the crystal is not insulating. Some of these may annihilate two pairs at a time, but one pair always remains. In general the number of pairs

of Weyl points and the sum of the $n_o(\boldsymbol{\kappa})$'s are both even or both odd.

A material with a single pair of Weyl points (the simplest case that can occur with $\sum_{\boldsymbol{\kappa}} n_o(\kappa)$ odd) would be an example of a Weyl semimetal, and would have some unusual type of conductivity. The Fermi energy would be forced to line up with the energy at the cone point, resulting in a density of states equal to zero. Assuming the material is not doped, the area of all electron-like Fermi surfaces has to cancel the area of the hole-like Fermi surfaces (due to the Lüttinger theorem). Thus, if there is only one pair of Weyl points, the Fermi energy cannot move away from zero, since it would then intersect the cones in small Fermi spheres containing the same type of carrier. This phenomenon does not occur if time reversal and inversion symmetry are both present, since a Weyl point is not invariant under the product of the symmetries (its chirality is reversed by them). Weyl points can also occur when $n_o(\boldsymbol{\kappa})$ is even[13], but in that case more symmetry would be necessary to pin the Fermi energy to them (since there would be additional pairs of Weyl points).

The stability of the Weyl points is explained in part by the basic result on degeneracies of eigenvalues, rather than by symmetry: in order to tune a Hamiltonian to a point where there is a degeneracy, three parameters are sufficient. Since $H(\mathbf{k})$ is a function of three momenta, these may be tuned to a point where there is a degeneracy, provided H is close enough to having a degeneracy in the first place.

Any set of parities $n_o(\boldsymbol{\kappa})$ satisfying $\prod_{\boldsymbol{\kappa}} \eta_{\boldsymbol{\kappa}} = 1$ can be realized in an insulator. There is never a direct phase transition (even with fine tuning) between two such phases when two or more $\eta_{\boldsymbol{\kappa}}$'s flip sign. When two modes cross at one TRIM in order to change the value of n_o there, Weyl points will form, and the system will be a semimetal. The Weyl points must then move to the second TRIM and reannihilate, so that the system becomes an insulator again, as illustrated in Fig. 5. There can be direct transitions where the value of n_o at a single TRIM changes by 2. However, such transitions are always fine-tuned, because two states above and below the Fermi energy have to switch places all at once.

The alternative argument for the presence of Weyl points when Eq. (4) is violated does not involve changing the Hamiltonian around and following its evolution. Instead, it is based on studying the Bloch states as a function of $\mathbf{k}$. Let us first suppose there is a single occupied band $|\psi_{1\mathbf{k}}\rangle$. To determine whether the wave function is even or odd, let us take its overlap with an even orbital $|s\rangle$ centered on the origin, $s_1(\mathbf{k}) = \langle s|\psi_{1\mathbf{k}}\rangle$. Plot the solutions in the Brillouin zone to

$$s_1(\mathbf{k}) = 0 \qquad (17)$$

This equation is a complex equation, amounting to two equations in three variables, so its solutions are curves. At a TRIM, $\psi_{1\boldsymbol{\kappa}}(\mathbf{r})$ is either even or odd. If it is odd, its overlap with $|s\rangle$ vanishes. Generically, if it is even,
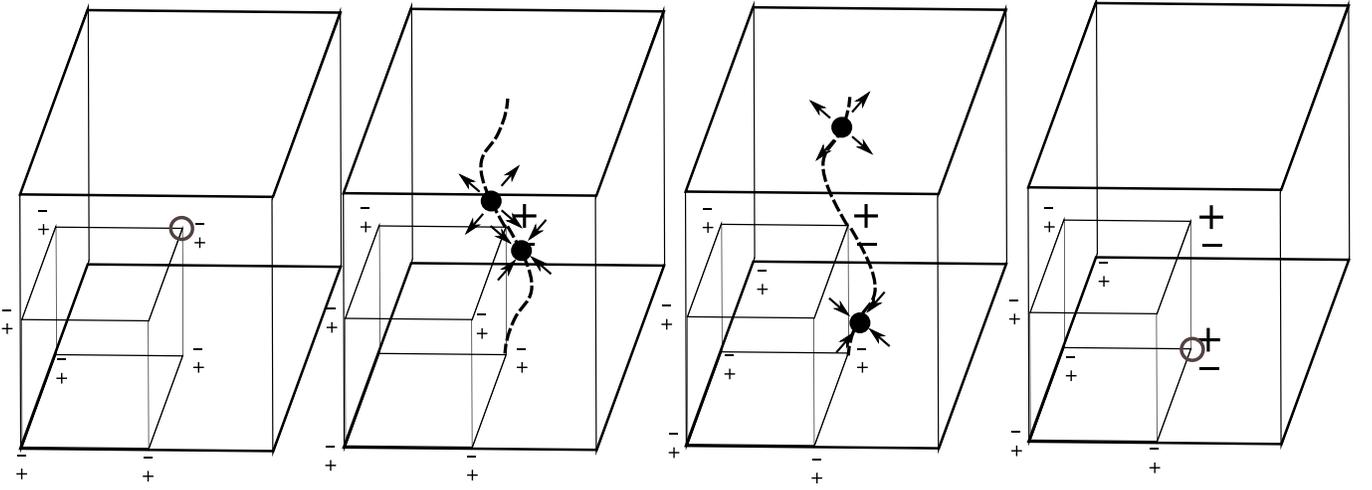
FIG. 5: Changing the parities of bands at two TRIMs. The figures represent the Brillouin zone of a system with two bands, one of which is filled. Initially, all the filled bands have parity +1, but the parities at two points are changed with the assistance of Weyl points which also act as monopoles in the Berry flux (see appendix D). A pair of monopoles forms at one TRIM and they move to another TRIM where they annihilate. In the process, the parities of the states at both TRIMs are reversed. The open circles indicate where the monopoles start out and disappear.
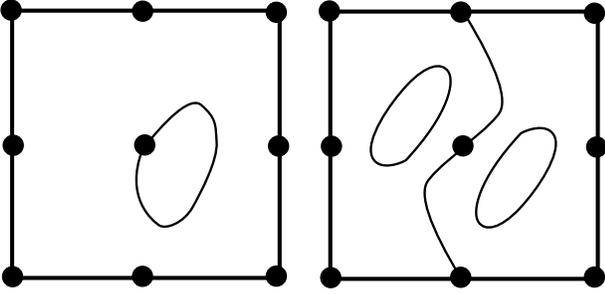

FIG. 6: Curves which are inversion symmetric must pass through an even number of TRIMs. Left, an attempt at drawing a curve that passes through one TRIM fails to be inversion symmetric. Right, an inversion symmetric figure; if there is just one curve passing through one of the TRIMs, it must go all the way around the Brillouin zone and pass through another TRIM on the way.

the overlap does not vanish. Hence, there is one curve through each TRIM at which $|\psi_{1\boldsymbol{\kappa}}\rangle$ is odd.

But since the curves are inversion symmetric, they must pass through an even number of TRIMs (see Fig. 6). Hence, the total number of TRIMs where $\mathcal{I}\psi_{1\boldsymbol{\kappa}} = -\psi_{1\boldsymbol{\kappa}}$ is even.

When there are several filled bands which do not touch each other, $\prod_{\boldsymbol{\kappa}} \eta_a(\boldsymbol{\kappa}) = 1$ for the ath band separately, and $\prod_{\boldsymbol{\kappa}} \eta_{\boldsymbol{\kappa}} = 1$ follows. If bands do touch, another step is required to see that the product is still one, even though the product for a single band may be -1. Consider the curves determined by $s_a(\mathbf{k}) = \langle s|\psi_{a\mathbf{k}}\rangle = 0$ for all the occupied bands $1 \leq a \leq n$. Some of these curves may be open arcs; they may end at a Weyl point between band

a and band $a \pm 1$ because $s_a(\mathbf{k})$ becomes discontinuous there. If that occurs, then there is always an arc leaving the Weyl point in the other band (see App. D). Putting all the arcs from the occupied states together therefore produces a set of closed curves; these curves will be variegated if the arcs in each band are imagined to have different colors, but they are still closed. Hence we can still deduce that they pass through the TRIMs an even number of times total, i.e., $\sum_{\boldsymbol{\kappa}} n_o(\boldsymbol{\kappa})$ is even.

B. Polarization and Hall Conductivity

Next, we interpret the u indices, showing that $u_{xy} \equiv \frac{\tilde{G}_{Hz}}{2\pi} \ (mod \ 2)$. This result is equivalent to Eq. (5) and applies to 14 of the remaining types of phase.

We will prove Eq. (5) momentarily, but it is logically necessary to derive the expression for the electrostatic polarization in one dimension first. The polarization is not captured by the AB_{31} crystal because it is not a *response* property. (With polarization taken into account, there are actually 8×32 different types of behavior that can occur in inversion symmetric phases.) Both polarization and the Hall coefficient can be expressed in terms of to the Berry connection, a vector function in momentum space. For a single band, the Berry connection is defined by

$$\mathbf{A}_a(\mathbf{k}) = i\langle u_{a\mathbf{k}}|\nabla_{\mathbf{k}}|u_{a\mathbf{k}}\rangle \qquad (18)$$

and the total Berry connection $\mathbf{A}(\mathbf{k})$ is the sum of the Berry connections of the occupied bands.

Consider a crystal in one dimension. We will prove that the intrinsic polarization is given (modulo e times a lattice vector) by Eqs. (7),(8) starting from the formula

in Ref. 14 for the intrinsic polarization of an arbitrary crystal, namely

$$P = P_e - \sum_i Z_i e(x_i - x_0). \tag{19}$$

The second term is the polarization of the nuclei in the unit cell relative to an origin, x_0, and the first term is the polarization of the electrons relative to x_0. Since the electrons are delocalized, calculating the latter contribution is subtle. It is given by

$$P_e = \frac{e}{2\pi} \sum_a \int dk A_a(k). \tag{20}$$

This expression for the polarization is ambiguous up to multiples of e, as expected on account of surface charge. For example if the unit cell is redefined, some nuclei locations are shifted by one unit changing the second term of Eq. (19). Likewise if the Bloch wave functions are redefined by $u_{ak} \rightarrow e^{i\theta(k)}u_{ak}$, then the polarization shifts by $\frac{e}{2\pi}(\theta(2\pi) - \theta(0))$, an integer multiple of e if $e^{i\theta(k)}$ winds around the unit circle.

To evaluate the polarization of an insulator with inversion symmetry, set $x_0 = 0$, the inversion center. First, consider a single band. The wavefunctions at k and $-k$ must be the same up to a phase, so $\psi_{-k} = e^{i\theta(k)}\psi_k$ for some phase $\theta(k)$. Therefore, $A(k) + A(-k) = \theta'(-k)$. Combining k and $-k$ together in Eq. (20) leads to $\tilde{P}_e = \frac{1}{2\pi}\int_0^\pi \theta'(-k)dk = \frac{1}{2\pi}(\theta(-\pi) - \theta(0))$. Now $e^{i\theta(k)}$ is the parity of the wave function ± 1 at TRIMs $k = 0, \pi$. Hence if the parities at the TRIMs are different, θ changes from 0 to π so $\tilde{P}_e \equiv \frac{1}{2}$ (mod 1). If there are many bands, we may sum the polarization over all of them and we find in general that

$$(-1)^{2\tilde{P}_e} = \eta_0 \eta_\pi. \tag{21}$$

The formula for the polarization in three dimensions can be deduced from this result–this is shown in detail below.

Now let us consider the Chern number for a *two* dimensional system, $H(k_x, k_y)$, and show that $(-1)^{\tilde{G}_{Hz}} = \prod_\kappa \eta_\kappa$. This is the two-dimensional version of Eq. (5). The Hamiltonian leads to a 1-D Hamiltonian H_{k_y} when k_y is fixed. As k_y changes, the polarization $P(k_y)$ of the one dimensional system changes. This means current must flow from one end to the other. According to Thouless's pumping argument, the Hall conductivity $\tilde{G}_{Hz}$ is equal to the total charge (divided by e) that flows in the 1D material when k_y changes by 2π. (In real space, the one-dimensional system is just the two-dimensional system rolled into a tube along the y direction. Changing k_y corresponds to applying an EMF for a period of time around the y-direction. Hence the Hall effect implies that charge should flow.)

Thus $\tilde{G}_{Hz} = -\frac{1}{e}\int_{-\pi}^\pi dP(k_y)$. (The polarization is not single-valued if $\tilde{G}_{Hz} \neq 0$.) Now if $\prod_\kappa \eta(\kappa) = -1$ (as in either of the 2D layers in Fig. 1 b) then the polarizations

at $k_y = 0$ and $k_y = \pi$ differ by a half integer. Thus, $\int_0^\pi dP = (k + \frac{1}{2})e$. By inversion symmetry, $dP(k_y) = dP(-k_y)$ (P is an odd function so dP is even). Hence the full change in the polarization between 0 and 2π is $2(k + \frac{1}{2})e$ and the Hall coefficient is odd, $\tilde{G}_{Hz} = -(2k + 1)2\pi$.

This section concludes with the generalizations of these results to three dimensions. The expression for the Hall coefficient in three dimensions Eq. (5) is basically a restatement of the two-dimensional result. Each of the three components of $\mathbf{G}_H$ is equal to the two-dimensional Hall coefficient for any cross-section of the Brillouin zone:

$$\begin{aligned} G_{Hz} &= \int \frac{dk_z}{(2\pi)} G_{Hz}^{2d}(k_z) \\ &= G_{Hz}^{2d}(k_{z0}) \end{aligned} \tag{22}$$

since the Chern number for any cross-section $k_z = k_{z0}$ is the same, because varying k_z is like taking a two-dimensional system and deforming it continuously. The Hall coefficient can be obtained modulo 2 by looking at an inversion symmetric plane, either $k_z = 0$ or $k_z = \pi$, giving Eq. (5). (Note that this gives another reason for the constraint $\prod_\kappa \eta_\kappa = 1$: the two planes have to agree about $\tilde{G}_{Hz}$'s parity.)

The expression for the Hall coefficient can be understood also by studying the evolution of the Hamiltonian from a frozen one into one with the parities $\mathbf{m_{xy}}$ and studying the monopoles in the intervening semimetallic phase, as in Fig. 5. When the monopoles move from $(\pi, \pi, 0)$ through the Brillouin zone to (π, π, π) where they annihilate, they leave behind a magnetic flux, so the Chern number is 2π. In this process, the parities flip on the edge parallel to the flux; hence the product of η_κ on either of the perpendicular faces is -1.

Now consider the polarization in three dimensions, which is given by $\mathbf{P}_e = e \iiint \frac{d^3}{\mathbf{k}}(2\pi)^3 \sum_a \mathbf{A}_a(\mathbf{k})$. For the polarization in three dimensions to be well-defined, $\mathbf{G}_H$ must be 0, so that there are no surface modes. According to Eq. 7, the pattern of signs is then a plane wave; in this situation all the 1d polarizations at TRIMs, $P_{1d}^x(\kappa_y, \kappa_z)$, are the same. This value in fact coincides with the three dimensional polarization. For example, in Fig. 1d. each of the four vertical lines through TRIMs looks like a one-dimensional insulator with half-integer polarization, so the net polarization per unit cell of the three-dimensional crystal is also $\frac{e}{2}\mathbf{R}_3$.

In more detail, the three-dimensional polarization is the integral over one-dimensional polarizations, $P^x = \iint \frac{dk_y dk_z}{(2\pi)^2} P_{1d}^x(k_y, k_z)$, if $G_{Hy} = G_{Hz} = 0$. (This condition ensures that P^x is single-valued.) The integrand is not a constant, but by inversion symmetry $P_{1d}^x(k_y, k_z) - P_{1d}^x(0, 0) = -(P_{1d}^x(-k_y, -k_z) - P_{1d}^x(0, 0))$. (Intuitively, one expects $P_{1d}^x(k_y, k_z)$ to be an odd function, but only differences in polarization are inversion symmetric because of the ambiguity in the polarization.) Hence $P^x = P_{1d}^x(0, 0)$, proving Eqs. (7) and (8).

Note that if $\mathbf{G}_H$ is nonzero, then part of the polarization is still well-defined. If $\mathbf{G}_H$ is parallel to $\hat{\boldsymbol{x}}$ (or in a non-cubic lattice, $\mathbf{g}_1$) then the x-component of the polarization cannot leak through the surface modes. On a cylindrical sample of material whose axis is along the x-direction of the crystal, the chiral modes circle around the cylinder, so they do not provide a short circuit between the two ends which would have allowed the x polarization to leak out. This component of the polarization is still given by Eqs. (7),(8).

The relationships we have proved so far give the physical interpretation of u and w modulo 2. They also have another meaning: they complete the problem of listing all the phases, by showing which combinations of the 11 integers $\mathbf{G}_H$ and $n_o(\boldsymbol{\kappa})$ occur in insulating materials. The 11 integers cannot be chosen independently (unlike the three Chern numbers in the non-symmetric classification); they must satisfy Eq. (4) and Eq. (5).

C. Magnetoelectric Response

Now we justify the relation $\theta = \pi \frac{1}{2} \sum_{\boldsymbol{\kappa}} n_o(\boldsymbol{\kappa})$ (Eq. (6)), for insulators with $\mathbf{G}_H = 0$, by calculating θ for a special case, $\mathbf{n_o} = 2\boldsymbol{m}_{xyz}$. This is the only nontrivial point in the unit cell of the eight dimensional classifying-crystal that is consistent with the conditions that the material is insulating and has no Hall conductivity, so any other case can be related to this one by deforming the insulator, and adding and subtracting frozen insulators to it. It is not possible to define θ for materials that have a Hall conductivity: for example, if θ is defined as $\frac{dP}{dB}$, the surface states interfere with defining P.

Now we need to show that $\theta = \pi$ for $2\mathbf{m_{xyz}}$. An insulator with the parities $2\mathbf{m_{xyz}}$ can be deformed to one with time reversal symmetry since the number of odd states at *each* TRIM is even (consistent with Kramers's theorem).

However, the time-reversal symmetry is a red herring when studying the magnetoelectric response, and so we will give an alternative argument. To calculate θ for $\mathbf{n_o} = 2\mathbf{m_{xyz}}$, it is enough to consider systems with two filled bands and the appropriate parities. (Any insulator with any additional bands, which would have to be even at all the TRIMs, has the same value of θ because they can be obtained by adding frozen bands.) The expression for θ in terms of the Berry connection[3,4,32] can be evaluated directly for the insulator with two bands using symmetry, similar to how the polarization was obtained above. The evaluation of this integral follows closely Ref. 33's calculation for the time-reversal-symmetric case. The first half of the argument for the time-reversal case applies to systems with inversion symmetry also, and leads to

$$\frac{\theta}{\pi} = \frac{1}{24\pi^2} \iiint d^3\mathbf{k}\,\epsilon^{ijk}(B^\dagger\partial_i B B^\dagger \partial_j B B^\dagger \partial_k B) \quad (23)$$

where $B_{a_1 a_2}(\mathbf{k}) = \langle u_{a_1}(-\mathbf{k})|I|u_{a_2}(\mathbf{k})\rangle$ and $u_a(\mathbf{k})$ is a pair of two wave functions spanning the occupied states

(it might not be possible to take these as energy eigenfunctions, since $u_a(\mathbf{k})$ have to be continuous, and energy eigenfunctions are not continuous when the bands touch each other). The *spaces* of occupied states are symmetric under inversion symmetry. $B(\mathbf{k})$ measures how far the wave functions chosen as a basis for them are from being inversion-symmetric, just as $e^{i\theta(k)}$ measures the asymmetry for a single wave function in the calculation of the one dimensional polarization. In a nontrivial phase, it is not possible to choose the basis functions in a continuous way without breaking the symmetry.

Now $B(\mathbf{k})$ gives a map from the Brillouin zone (a three-dimensional torus) to SU_2 (also three-dimensional). The expression above for $\frac{\theta}{\pi}$ is known to equal the degree of this map, i.e., the number of times the torus covers SU_2. The degree of the map modulo 2 is the number of solutions to $B(\mathbf{k}) = -\mathbb{1}$ (or any fixed matrix). We may just count the TRIMs satisfying this condition, because all other solutions come in pairs at $\mathbf{k}$ and $-\mathbf{k}$ (since inversion symmetry implies $B(-\mathbf{k}) = B^\dagger(\mathbf{k})$), and the number of TRIMs where B has this value is determined by $\mathbf{n_o}$.

We have found that only *some* combinations of the n_o parameters modulo 2 and 4 have physical interpretations. In the next section, we will see that all the n_o-parameters do have interpretations in the entanglement spectrum. This will give another perspective on why only values of the n_o modulo 4 are important: the entanglement modes cannot be observed directly. However, numbers of entanglement modes modulo 2 are related to various observable properties.

V. PARITIES AND THE ENTANGLEMENT SPECTRUM

The relations between the properties of the insulator and the parities can be derived geometrically using the entanglement spectrum of the insulator; there is a rule for counting the number of states in this spectrum based on the parities.

The entanglement spectrum measures quantum correlations in the ground state of a system (see e.g. Ref. 24). It is defined using the Schmidt decomposition. The insulator is cut by an imaginary plane passing through a center of inversion symmetry. The many-body ground state wave function then decomposes,

$$|\Psi\rangle = \frac{1}{\sqrt{Z}} \sum_\alpha e^{-\frac{E_\alpha^e}{2}} |\alpha\rangle_L |\alpha\rangle_R. \quad (24)$$

where Z is a normalization constant and E_α^e controls the weight of a given term. It is called the entanglement "energy" because the probability of each term is given by the Boltzmann distribution. The states $|\alpha\rangle_L$ are called the entanglement states, and they are analogous to the surface states of the half of the system on the left side of the cut.

When the wave function of the entire system is a free system described by a Slater determinant, the entangle-

ment states $|\alpha\rangle_L$ are Slater determinants, too[24]. They are formed just like the excited states of a system of free electrons, by selecting wave functions from a certain orthonormal family of single-particle wave functions $f_{i\mathbf{k}_\perp}^L(\mathbf{r})$. (These states may be labelled by the momentum along the surface, $\mathbf{k}_\perp$, by translational symmetry.) Each of these wave-functions has an associated "energy" $\epsilon_{Li}(\mathbf{k}_\perp)$ as if they were eigenfunctions of a single-particle Hamiltonian. The entanglement "energy" E_α^e is the sum of all the "energies" of the occupied states.

The entanglement spectra, $\epsilon_{Li}(\mathbf{k}_\perp)$, can be used to determine "topological" properties of a system. When a material is insulating in the bulk, it may still have a gapless entanglement spectrum. This implies that electrons are delocalized across the cut, unlike the electrons in a frozen insulator. These delocalized states may be "topologically nontrivial." Physical topological surface states can be deduced from such entanglement spectrum states: the entanglement spectrum can be continuously deformed into the physical spectrum, so any topologically protected states are present in both[17,18].

Determining basic properties of the entanglement spectrum is simple in the presence of inversion symmetry. In this case[18], the entanglement spectrum has a particle-hole symmetry $\mathcal{I}_e$ that implies a rule for finding the number of entanglement states at each surface TRIM. The $\mathcal{I}_e$ symmetry takes each mode to another mode whose momentum $\mathbf{k}_\perp$ and "energy" $\epsilon_{Li}(\mathbf{k}_\perp)$ have the opposite sign. Let us regard 0 as the Fermi "energy"; the state in the Schmidt decomposition with the smallest "energy" (i.e., the largest weight) is obtained by filling up all states with $\epsilon_{Li} < 0$.

At surface TRIMs $\mathcal{I}_e$ ensures that states appear in pairs with energies $\pm\epsilon$ when $\epsilon \neq 0$. There can be a single mode at zero. If present, this mode will stay exactly at zero no matter how the system is changed, because moving away would break the symmetry. More can be said about the zero-energy states: the "index" at each TRIM can be determined. The space of zero-"energy" states is invariant under $\mathcal{I}_e$ so they can be classified by their parities. The index is the difference $\Delta N_e(\boldsymbol{\kappa}_\perp)$ between the number of modes of even and odd parity. This quantity is invariant because even and odd zero-energy states can "cancel" one another and move to nonzero energies $\pm\epsilon$, while two states of the same parity cannot cancel. (If two states move away from zero energy, then they must turn into eigenstates f_1 and f_2 with energies of opposite sign. Thus, f_1 and f_2 are orthogonal states exchanged by $\mathcal{I}_e$. The corresponding parity eigenstates, $\frac{1}{\sqrt{2}}(f_1 \pm f_2)$, have opposite parities.) Thus, if $\Delta N_e(\boldsymbol{\kappa}_\perp)$ has some value, such as 2, then there must be at least 2 states at this TRIM.

The imbalance number can be found directly from the bulk band structure,

$$\Delta N_e(\boldsymbol{\kappa}_\perp) = 1/2(\Delta N(\boldsymbol{\kappa}_1) + \Delta N(\boldsymbol{\kappa}_2)) \qquad (25)$$

where $\boldsymbol{\kappa}_1$ and $\boldsymbol{\kappa}_2$ are the two bulk inversion-symmetric momenta that project to $\boldsymbol{\kappa}_\perp$ and $\Delta N(\boldsymbol{\kappa}_1)$ (e.g.) is related

to $n_o(\boldsymbol{\kappa}_1)$: it is the difference between the number of even and odd occupied states at $\boldsymbol{\kappa}_1$, that is $n - 2n_o(\boldsymbol{\kappa}_1)$. This result applies in any dimension. In one dimension, for example, there is only one ΔN_e (since there is only one surface momentum) to determine, and ΔN_e *is equal to the number of even states at $\kappa = \pi$ minus the number of odd states at $\kappa = 0$.* Note that the parities of the bulk states are to be calculated relative to an inversion center that is on the cutting plane[34].

We will now explain how to define the particle-hole symmetry and how to derive the formula for ΔN_e. This derivation requires some results of Refs. 24,35 whose derivations are summarized in appendix E. As the building-up of entanglement states from single-particle states suggests, the entanglement modes are actually eigenfunctions of a "Hamiltonian" H_L defined on the part of space to the left of the cutting plane. The eigenvalues of H_L are not equal to the entanglement energies ϵ_{Li}, but they are related to them,

$$H_L|f_{i\mathbf{k}_\perp}^L\rangle = \frac{1}{2}\tanh\frac{1}{2}\epsilon_{Li}(\mathbf{k}_\perp)|f_{i\mathbf{k}_\perp}^L\rangle.$$

The Hamiltonian H_L is just the result of confining the "flat-band Hamiltonian" H_{flat} in the whole space to the left half of space. H_{flat} is defined to have the same eigenfunctions as the true Hamiltonian but simpler eigenvalues, $-\frac{1}{2}$ for the occupied states and $+\frac{1}{2}$ for the empty ones. H_L has strange eigenstates–it has infinitely many surface bands, and for many cases, it has no states besides these. The reason is that the spectrum of H_L ranges from $-\frac{1}{2}$ to $\frac{1}{2}$. Each bulk state has an energy exactly equal to $\pm\frac{1}{2}$ (corresponding to $\epsilon_{Li} = \pm\infty$) so any state with a finite ϵ_{Li} is a surface state.

While H_L is obtained from H_{flat} by cutting off the right half of space, cutting away the left half of the space leads to a partner Hamiltonian H_R (whose eigenfunctions f_R generate the Schmidt states on the right). These three Hamiltonians have unusual interconnections that do not occur when a generic Hamiltonian is "cleaved" by just confining it to half of space. For example, many eigenstates of H_{flat} give eigenstates of H_L and H_R when the wavefunction is set to zero in the part of space that is being discarded. For a generic Hamiltonian, the wave function on the remaining half of the space would be depleted near the surface. The unusual relationships between the eigenfunctions of these three Hamiltonians follow because H_{flat} satisfies an identity $H_{flat}^2 = \frac{1}{4}$.

The connections between the eigenstates of the three Hamiltonians are as follows. The eigenfunctions of H_L and H_R are in one-one correspondence via a map $\mathcal{M}$. This map reverses the sign of the "energy." Furthermore, it is possible to build up a complete set of occupied states of H_{flat} from these pairs:

$$F_{i\mathbf{k}_\perp}(\mathbf{r}) = \sqrt{\frac{1}{2}\text{sech}\frac{\epsilon_{Li}(\mathbf{k}_\perp)}{2}} \times$$
$$\left[e^{-\frac{1}{4}\epsilon_{Li}(\mathbf{k}_\perp)}f_{i\mathbf{k}_\perp}^L(\mathbf{r}) + e^{\frac{1}{4}\epsilon_{Li}(\mathbf{k}_\perp)}\mathcal{M}f_{i\mathbf{k}_\perp}^L(\mathbf{r})\right]. \qquad (26)$$

This is an occupied state since applying H_{flat} to it gives an eigenvalue of $-\frac{1}{2}$. As f_i^L varies over *all* eigenstates of H_L, the function F varies over a basis for the *occupied* states in the ground state. These states are strange eigenstates for a bulk Hamiltonian since they are localized; this is possible because wave packets do not move in H_{flat}: the group velocity is zero since the dispersion is flat. (Another curiosity of these partnered wave functions is that the weights in the superposition depend on the energy.)

When the system is inversion symmetric, $\mathcal{M}$ and $\mathcal{I}$ can be combined together to give the symmetry $\mathcal{I}_e$; it is a transformation within the left half of the insulator, defined by $\mathcal{I}_e = \mathcal{IM}$. Since $\mathcal{I}$ is a symmetry of the wave function, it preserves ϵ while $\mathcal{M}$ reverses its sign. Therefore, $\mathcal{I}_e$ acts as a particle-hole symmetry. Similarly, $\mathcal{I}_e$ also reverses the sign of $\mathbf{k}_\perp$.

Now we can count the zero entanglement-"energy" states at TRIMs. Let us call the parities of these states under $\mathcal{I}_e$ "$\eta_{i\boldsymbol{\kappa}_\perp}^e$." A state $f_{i\boldsymbol{\kappa}_\perp}^L$ with this parity extends, by Eq. (26), to an occupied state

$$F_{i\boldsymbol{\kappa}_\perp} = \frac{1}{\sqrt{2}}\left[(f_{i\boldsymbol{\kappa}_\perp}^L(\mathbf{r}) + \eta_{i\boldsymbol{\kappa}_\perp}^e f_{i\boldsymbol{\kappa}_\perp}^L(-\mathbf{r})\right]. \qquad (27)$$

where we have used $\mathcal{IM}f_{i\boldsymbol{\kappa}_\perp}^L = \eta_{i\boldsymbol{\kappa}_\perp}^e f_{i\boldsymbol{\kappa}_\perp}^L$ to relate f^R to f^L. This state is invariant under ordinary inversion, and the parity is $\eta_{i\boldsymbol{\kappa}}^e$.

Let us determine the value of ΔN_e for a one-dimensional system. The result in higher dimensions follows since we can fix $\mathbf{k}_\perp = \boldsymbol{\kappa}$ to obtain a one-dimensional system. Consider a circular chain with an even number of cells, L. Now, count the number of even occupied states W_e minus the number of odd occupied states W_o, using two different bases. $W_e - W_o$ is equal to tr $\mathcal{I}$ so it is the same in both bases; the equality will be Eq. (25).

One orthonormal basis will be obtained by cutting the system along a diameter. There will now be two cutting points 0 and $\frac{L}{2}$. Near each of these cuts are localized an orthonormal set of F states (Eq. (26)). The two sets (plus bulk states if any exist) together form a full basis for the wave functions on the ring. The zero-"energy" states give parity eigenstates centered on each of the two cuts, according to Eq. (27). These contribute $2\Delta N_e$ to $W_e - W_o$. The remaining states do not contribute because they can be organized into inversion-related pairs, $F_i(x), F_i(-x)$. These states states are all mutually orthonormal because their left and right halves correspond to different eigenvalues of H_L, H_R. The inversion matrix $\mathcal{I}$ has only off-diagonal matrix elements between $F_i(x)$ and $F_i(-x)$.

On the other hand, instead of the localized wavefunctions, we can use the extended Bloch functions, $\psi_a(k_x)$. The wave functions at momentum $\pm k_x$ do not contribute to the trace of $\mathcal{I}$ because they are exchanged, while the wave functions at the TRIMs contribute $(\Delta N(\pi) + \Delta N(0))$ to $W_e - W_o$. Setting the two expressions for tr$\mathcal{I}$ equal to each other gives Eq. (25).
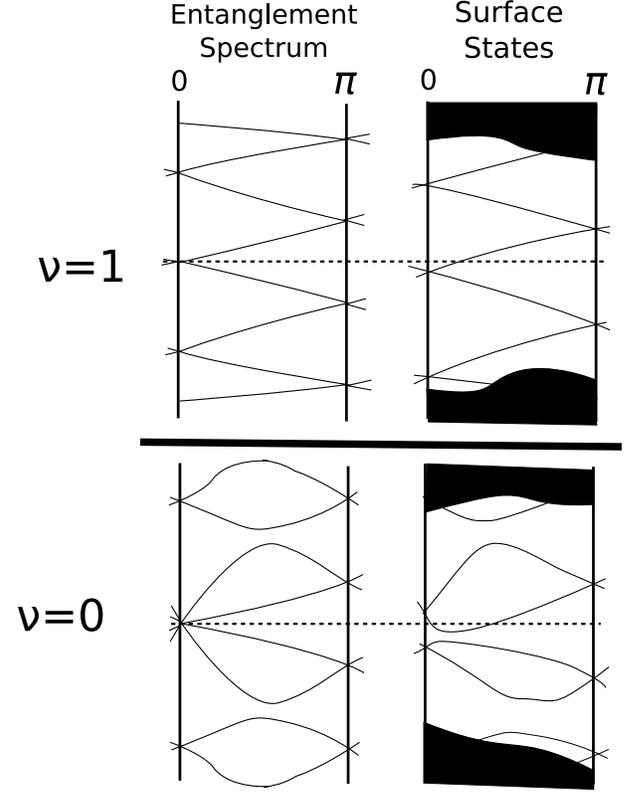

FIG. 7: Determining the Quantum Spin Hall index using the entanglement spectrum. The figure compares spectra of a nontrivial and a trivial system. The left spectrum for each system is the entanglement spectrum, and the right illustrates how the surface spectrum might look. In the entanglement spectrum, inversion symmetry protects degeneracies at zero energy at the TRIMs, allowing one to determine the index. But the two sets of spectra can be deformed into one another (the difference is probably more drastic than illustrated). Because time reversal symmetry produces Kramers degenereacies at the TRIMs at all energies, the parity of the number of modes crossing the Fermi energy does not change.

We can now count the entanglement states of a two-dimensional insulator to understand their *physical* surface properties. For example, applying the result to an insulator that has both time reversal and inversion symmetry gives a simple derivation of the the formulae from Ref. 10 for the indices of topological insulators. We will focus on the two dimensional quantum spin-Hall index, since the three dimensional indices are defined in terms of it. The quantum spin-Hall index ν is the number (modulo 2) of physical edge modes betweeen 0 and π. As we have just seen, finding states in the entanglement spectrum is easy because of the particle-hole symmetry (see Fig. 7). Once these are found in the entanglement spectrum, they remain when it is deformed into the physical spectrum, by the standard arguments.
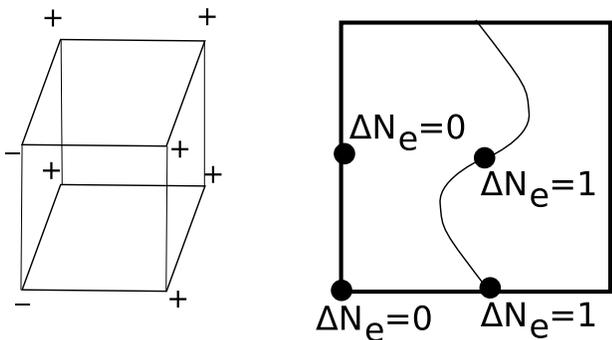
FIG. 8: A model with a single filled band that has an odd quantum Hall effect parallel to $\mathbf{R}_z$. a) The parities at the TRIMs. b) The entanglement states on the xz-face of the Brillouin zone, determined using $\Delta N_e(\boldsymbol{\kappa}_\perp) = \frac{1}{2}(\Delta N(\boldsymbol{\kappa_1}) + \Delta N(\boldsymbol{\kappa_2}))$.
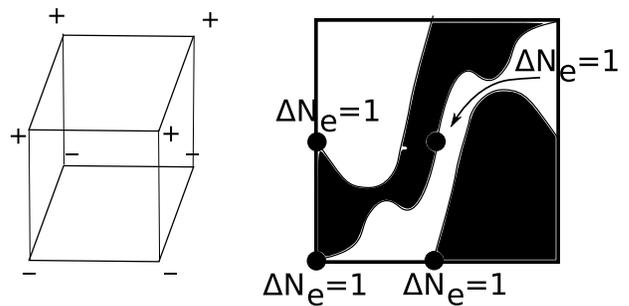

FIG. 9: Determining the polarization from the entanglement spectrum. a) Parities for an insulator with one filled band, with a half-filled Fermi sea in the entanglement spectrum. b)Possible entanglement Fermi arcs for a cut parallel to the xz plane. The arcs surround half the surface Brillouin zone. If there are no nuclei on $y = 0$, this crystal has a half-integer polarization in the y-direction.

Consider the entanglement spectrum created by dividing the system at $y = 0$. The spin Hall index is the parity of the number of curves in the dispersion $\epsilon(k_x)$ crossing $\epsilon = \text{const.}$ between $k_x = 0$ and π. Consider in particular the axis $\epsilon = 0$. Strictly between 0 and π the axis crosses an even number of modes: the crossings come in pairs because the spectrum is symmetric under $\mathcal{TI}_e$, which just flips the sign of ϵ. (Generically, these states will just mix and move off the axis.)

Therefore only the modes at the ends of the interval are important. We may assume that all the modes at either of these TRIMs have the same parity, because otherwise the states whose parity is in the minority may combine with the states in the majority and become gapped. Then by Eq. (25) the number of modes at, e.g., $k_x = 0$ is

$$|\Delta N_e(0)| = |n - n_o(0,0) - n_o(0,\pi)|. \qquad (28)$$

Since these modes are at the extremes of the interval from 0 to π, each one only qualifies as half a mode. To justify this guess, look at a line slightly above the axis. This line crosses half of the modes emanating from each TRIM, so the number of crossings, mod. 2, is $\nu \equiv \frac{1}{2}\sum_{k_x=0}^{\pi}|n - n_o(k_x,0) - n_o(k_x,\pi)|$. This is congruent to $\frac{1}{2}\sum_{\boldsymbol{\kappa}} n_o(\boldsymbol{\kappa})$, summed over all four TRIMs, in agreement with the standard result.

When the flat band Hamiltonian is deformed into the true Hamiltonian, ν remains the same even though the surface states no longer have particle-hole symmetry. The energy curves form continuous loops or zigzags (see figure) because of the double-degeneracies protected by Kramers' theorem.

We can use a similar approach to understand the results in Sec. IV for the polarization and Hall coefficient. These effects may be determined by sketching the arcs of the entanglement Fermi surface using the information about the number of zero energy states at the TRIMs. While each zero energy state at a TRIM gives at least a Fermi point, not all of these points extend to Fermi arcs. Helpfully, the *parity* of the number of Fermi arcs

is the same as ΔN_e's parity though. (This is proved in appendix F.)

Fig. 8 shows how the modes might look for one set of parities. Consider the xz surface of this insulator. According to Eq. (25) there must be one arc (or an odd number) passing through $(\pi, 0)$ and (π, π), and an even number through the other two TRIMs. Minimally, there is only one Fermi arc, as illustrated in Fig. 8. Hence as one travels along k_x through the Brillouin zone, one crosses through the Fermi arc. Since the z-component of the Hall conductivity, $\tilde{G}_z$ is the number of arcs (counted with a sign depending on the sign of the group velocity), $\frac{1}{2\pi}\tilde{G}_{Hz} = \pm 1$. In more complicated cases, we can determine only that $\frac{1}{2\pi}\tilde{G}_{Hz}$ is odd because there may be Fermi arcs that do not pass through TRIMs. These cannot be predicted from the $n_o(\boldsymbol{\kappa})$ parameters, but they come in pairs by inversion symmetry, so the parity of the Hall coefficient is uniquely determined.

Now consider the parities in Fig. 9. One possible choice of modes (with one passing through each TRIM point as required) is illustrated. If these modes are not chiral, then they separate the Brillouin zone into filled and empty states; exactly half the Brillouin zone is filled because of the symmetry. This will imply that $P^y = \frac{e}{2}$ if there are no nuclei on $y = 0$, and this will be seen to agree with the rule for the polarization.

The polarization is defined as the surface charge once the surface bands have been emptied. (See appendix G.) This definition may be applied also to the entanglement spectrum. Cut the system with a plane $y = 0$ through a point of inversion symmetry. If there are no nuclei on this plane (which would be indivisible), then the plane just divides the electronic part of the wave function in two parts.

Of all the terms in the Schmidt decomposition, consider the one with the largest coefficient, $|G\rangle_L|G\rangle_R$, where $|G\rangle_L$ and $|G\rangle_R$ are the ground states of H_L and

H_R respectively, obtained by filling all the negative energy states. These states are mirror images of each other, so they both have the same surface charge Q_y. The net charge is $2Q_y$. However, the Schmidt state $|G\rangle_L|G\rangle_R$, obtained by collapsing the wave function by making a hypothetical measurement, has the same charge as the ground state. Each electron is pushed over to the side of the $y = 0$ plane where it is more likely to be, but no electrons appear or disappear. Thus, $2Q_y = 0$, i.e., the ground state of H_L has no surface charge.

Now Fig. 9 shows that this ground state of H_L has a partially filled band. When this band (which covers half the Brillouin zone) is emptied, a charge of $-\frac{e}{2}$ per unit cell on the surface remains. Hence the polarization $P^y \equiv \frac{e}{2} \pmod{e}$.

To compare this result to Eq. (8), we need to calculate both contributions to this equation, from nuclei and electrons. Note that $P_e^y = 0$ for the given parities. Since there is one filled band of electrons, by neutrality, there must be a single charge $-e$ nucleus per unit cell, which contributes $P_n^y = \frac{e}{2}$. (The nuclei must be at $y \equiv -\frac{1}{2}$ because these are the only inversion symmetric points that are not on the cutting plane.) Appendix G gives a more general argument.

We would also like to prove the rule for θ using the entanglement spectrum. The entanglement modes of such an insulator (see Fig. 2b) include a Dirac point. Such modes, if they were physical, would produce a half-integer Hall effect. However, this argument is incomplete since the entanglement modes are not physical.

VI. CONCLUSIONS

This study shows that, beyond the Chern numbers that can be used to classify insulators without symmetry, the only protected quantities for insulators with inversion symmetry are the parities of the occupied states at the TRIMs.

For bulk materials, certain values of the parities imply non-vanishing electrical properties (the reverse of the usual use of parity symmetry, to prove the vanishing of certain quantities). In particular, if the number of odd occupied states is odd, the material is never a complete insulator.

The parities also provide a simple criterion for determining when a crystalline compound has a magnetoelectric response equal to π, the generalization of the result on the strong topological index of an insulator with time-reversal symmetry as well as inversion symmetry. Hence, the magnetoelectric effect could occur in magnetic materials. There are two consequences: The magnetoelectric effect could be generated by the magnetic ordering, rather than spin-orbit coupling; thus there are more possible materials, besides ones containing elements with large Z's so that the electrons are spin-orbit coupled. It would be interesting to search for such a material. Second, in a material with spontaneous magnetism

and $\theta = \pi$, the magnetoelectric effect would be easier to observe than in a topological insulator, because the material does not have gapless surface states that would interfere with the observation.

Beyond these properties, the static polarization, and the Hall conductivities' parities, there are no independent response properties that are related to the inversion parities, since any two insulators which have these response properties in common can be deformed into one another, apart from some frozen electrons.

The properties of inversion symmetric insulators can be derived in a simple way with the help of the entanglement spectrum, illustrating how entanglement modes can be indirectly observed: a magnetoelectric response of $\theta = \pi$ corresponds to a material with an odd number of Dirac points in the entanglement spectrum (even when there are no surface states at all).

Understanding the stability of the parity invariants to interactions will be an interesting subject for future study. Ref. 36 shows in one dimension that phases can merge when interactions are turned on. In non-interacting systems, more complicated point groups may also protect more interesting phases. Perhaps there are even *new* types of quantized responses in these phases.

Appendix A: Tight Binding Models and Inversion Parity.

A useful set of models for studying inversion symmetric Hamiltonians are tight-binding models with one atom per unit cell which has some orbitals that are even, $|s_i\rangle$, where i ranges from 1 to N_{even} and some odd ones, $|p_i\rangle$, where i continues from $N_{even} + 1$ to $N_{odd} + N_{even}$. Let the Hamiltonian be

$$H = - \sum_{i,j,\mathbf{R},\boldsymbol{\Delta}} t_{ij}(\boldsymbol{\Delta}) c_i^\dagger(\mathbf{R} + \boldsymbol{\Delta}) c_j(\mathbf{R}), \qquad \text{(A1)}$$

where c_i includes creation operators for both types of orbitals.

A Bloch wave function $\psi_{a\mathbf{k}}$ (a is the band index) is determined by its values at the origin, ϕ_i, which are repeated in a plane-wave fashion to other sites. Inversion maps $\mathbf{k} \to -\mathbf{k}$ and $\phi_i \to I_{0ij}\phi_j$, where I_{0ij} is a diagonal matrix of N_{even} ones and N_{odd} minus ones.

There is a simple criterion for determining the parities of the occupied states at the TRIMs, in case one wants to determine the parities of states in a numerical band structure calculation using a basis of molecular orbitals,

for example: if a state is odd, then all its s-wave components vanish. If it is even, all p-wave components vanish. In the generic case, it is enough to check a single s-wave component:

$$\eta_a(\boldsymbol{\kappa}) = +1 \text{ if } \langle s_1|\psi_{a\boldsymbol{\kappa}}\rangle \neq 0$$
$$\eta_a(\boldsymbol{\kappa}) = -1 \text{ (probably) if } \langle s_1|\psi_{a\boldsymbol{\kappa}}\rangle = 0. \qquad \text{(A2)}$$

If a component is exactly zero, it is reasonable to assume that it is because inversion symmetry forbids that component.

The Hamiltonian used to illustrate the entanglement-rule in Fig. 2 is of this type. In momentum space Eq. (A1) can be written $\sum_{ij} c_i^\dagger(\mathbf{k})c_j(\mathbf{k})H_{ij}(\mathbf{k})$. The Hamiltonian can be built from two subsystems H_1, H_2, whose occupied states are given by the upper and lower signs in Fig. 2. Each Hamiltonian can be gapped because both sets of signs satisfy the constraint $\prod_{\boldsymbol{\kappa}} \eta_{\boldsymbol{\kappa}} = 1$ by themselves.

Each of these Hamiltonians H_r can be constructed in a space with one even state $|s_r\rangle$ and one odd state $|p_r\rangle$. For the Hamiltonian to be inversion symmetric it must commute with σ_z, so the diagonal matrix elements are even and the off-diagonal matrix elements are odd functions of $\mathbf{k}$.

The two Hamiltonians can be combined together by including a small mixing between the two systems. The final Hamiltonian has the form:

$$H(\mathbf{k}) = \begin{pmatrix} H_1(\mathbf{k}) & t\mathbb{1} \\ t\mathbb{1} & H_2(\mathbf{k}) \end{pmatrix}. \qquad \text{(A3)}$$

where

$$H_1 = A_{\mathbf{k}}\sigma_z + B_{\mathbf{k}}\sigma_x + C_{\mathbf{k}}\sigma_y$$
$$H_2 = D_{\mathbf{k}}\sigma_z + E_{\mathbf{k}}\sigma_x + F_{\mathbf{k}}\sigma_y \qquad \text{(A4)}$$

and

$$A_{\mathbf{k}} = (1 - \cos(k_x))\cos(k_y) + (1 + \cos(k_x))\cos(k_y - k_z)$$
$$B_{\mathbf{k}} = (1 - \cos(k_x))\sin(k_y) + (1 + \cos(k_x))\sin(k_y - k_z)$$
$$C_{\mathbf{k}} = \sin(k_x), E_{\mathbf{k}} = -\sin(k_x), F_{\mathbf{k}} = \sin(k_z)$$
$$D_{\mathbf{k}} = \cos(k_x) + \cos(k_z) - 1.$$

The parities of the occupied states at $\boldsymbol{\kappa}$ of H_1 and H_2 under inversion in the point $\frac{1}{2}\hat{\boldsymbol{x}}$ are equal to the signs shown in Fig. 2. Choosing this point to define the inversion parities is necessary because the entanglement spectrum is obtained by cutting the system between two planes of the atoms.

Appendix B: Classification using Topology in the Space of Hamiltonians

In this section we will show how to use systematic methods from topology to classify the insulators with inversion symmetry. This method was also used to find the classification of topological phases with the Altland and Zirnbauer symmetry groups[15,16].

In general we write a band insulator as $H(\mathbf{k})$, which we think of as a vector bundle on the Brillouin zone. The eigenvectors of $H(\mathbf{k})$ with energies below the chemical potential are the occupied states, defining a vector subspace of the entire Hilbert space at $\mathbf{k}$. For inversion-symmetric insuators, there is an additional constraint on the Hamiltonian: $\mathcal{P}^0[H(\mathbf{k})] \equiv I_0 H(\mathbf{k}) I_0 = H(-\mathbf{k})$, this relates the Hamiltonians at $\mathbf{k}$ and $-\mathbf{k}$.

The idea behind our method of classification, similar to the one used for time-reversal invariant topological insulators, is to look only at half the Brillouin zone.

For a Hamiltonian H in d-dimensions, one can construct a path $f(t) = H(k_x = \pi t, k_2, k_3, \dots)$ in the space of $(d-1)$-dimensional Hamiltonians, where the endpoints $(t = 0, 1)$ are inversion symmetric. Thus the classification of d-dimensional Hamiltonians is equivalent to the classification of paths in $\mathfrak{P}(\mathcal{H}_{d-1}; \mathcal{I}_{d-1}, \mathcal{I}_{d-1})$, where $\mathcal{H}_d$ is the set of general d-dimensional Hamiltonians and $\mathcal{I}_d \subset \mathcal{H}_d$ is the subset which is inversion-symmetric. The symbol $\mathfrak{P}(X; A, B)$ is defined to be:

$$\mathfrak{P}(X; A, B) \equiv \text{Set of paths in } X \text{ from } A \text{ to } B \qquad \text{(B1)}$$
$$= \{f : [0, 1] \to X | f(0) \in A, f(1) \in B\},$$

where $A, B \subset X$. We want to divide up $\mathcal{I}_d$ into sets such that paths from different sets are not homotopic to each other. Heuristically, the classes of paths of $\mathfrak{P}(X; A, B)$ are given by the number of components of A, B which determines the set of possible endpoints, and the loop sturcture of X which determines the number of ways to travel from A to B. The classes of insulators in d-dimensions is very roughly given by:

Components of $\mathcal{I}_d$

$$\sim \frac{\text{Loops in } \mathcal{H}_{d-1}}{\text{Loops in } \mathcal{I}_{d-1}} \times (\text{Components of } \mathcal{I}_{d-1})^2. \qquad \text{(B2)}$$

This idea is made precise using algebraic topology[38], and is captured by an exact sequence below (B4) (which explains the reason for the denominator here).

There is an addition structure in the classification of insulators[38], which comes from the fact that one can combine two insulators together using direct sums "$\oplus$". To simplify the classification, it is useful to also have a subtraction "$\ominus$" operation between insulators. This would give the topological invariants (*e.g.* $\mathbb{Z}$) a group structure.

The subtraction procedure is realized by considering an ordered pair of bands (H_1, H_2), which represents the "difference" of the two Hamiltonians. Addition by H' is given by $(H_1 \oplus H', H_2)$ and subtraction is given by $(H_1, H_2 \oplus H')$. Imposing the equivalence relation $(H_1 \oplus H', H_2 \oplus H') \sim (H_1, H_2)$ makes the addition and subtraction processes cancel each other. Physically, we are interested in classifying difference of two topological insulators – this is analogous to studying domain walls between them whose properties are determined only by

the difference in topological invariants. With this interpretation, it is possible to talk about a negative number of filled bands (whenever H_2 has more bands than H_1).

The construction above, called the *Grothendieck group*, has two interpretations. First, two insulators H_1, H_2 are deformable to one another when the topological invariants of the band structure (H_1, H_2) are all trivial. Second, the invariants classifying phases of H can be defined as the topological invariants of (H, vac), where the second insulator is the vacuum.

1. Hamiltonians, Classifying Spaces and Homotopy Groups

Consider an $N \times N$ matrix H with n occupied states and $N - n$ empty states. Setting the chemical potential to be zero, H is a matrix with n negative eigenvalues and $N - n$ positive eigenvalues. In the topological classification of insulators, the energies are irrelevant so long as we can distinguish between occupied and unoccupied states, and hence we can deform the energies (eigenvalues) of all valence bands to -1 and the energies of conduction bands to $+1$. We can also assume there are an infinite number of conduction bands, and so we let $N \to \infty$. $\mathcal{H}_0$ is the set of such 0D Hamiltonians, and can be separated into discrete components based on the number of filled bands (which may be negative for *differences* of Hamiltonians). The space $\mathcal{H}_0$ is homeomorphic to $\mathbb{Z} \times BU$, where BU is the classifying space of the unitary groups.

At the TRIM, the Hamiltonian is inversion-symmetric and commutes with the operator I_0. The Hilbert space is divided into an even subspace and an odd subspace, based on the inversion eigenvalues. Hence the set of inversion-symmetric (0D) Hamiltonians $\mathcal{I}_0$ is homeomorphic to $\mathcal{H}_0 \times \mathcal{H}_0$.

Finally, we introduce the "vacuum" $v_0 \in \mathcal{I}_0 \subset \mathcal{H}_0$, which is a Hamiltonian with no filled bands. v_0 is a useful object in that it allows us to compare any Hamiltonian to it, and also acts as the basepoint when we compute the homotopy groups of $\mathcal{H}_0, \mathcal{I}_0$.

Given a topological space X and a basepoint within the space x_0, the *homotopy group* $\pi_s(X)$ is the set of equivalence classes of maps $f : (S^s, b_0) \to (X, x_0)$, where the basepoint $b_0 \in S^s$ and $f(b_0) = x_0$. For example, $\pi_0(X)$ gives the number of connected components of X, and $\pi_1(X)$ tells us which loops in X are equivalent and which loops are contractible.

The group strucutre of $\pi_s(X)$ is given by concatenation of maps. However, the group structure of the Hamlitonians has already been defined based on direct sums. Fortunately, the group composition defined based on the two methods (concatenation / direct sums) are equivalent.

The homotopy groups of $\mathcal{H}_d$ are known: $\pi_0(\mathcal{H}_0) = \mathbb{Z}$ because 0-dimensional Hamiltonians are classified by the number of filled bands n. $\pi_1(\mathcal{H}_0) = 0$ means that loops in $\mathcal{H}_0$ are all contractible. $\pi_2(\mathcal{H}_0) = \mathbb{Z}$, because
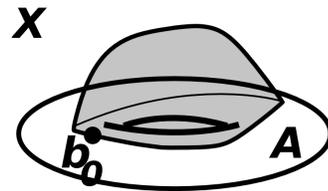

FIG. 10: Relative homotopy groups. The figure represents an element of $\pi_2(X, A, x_0)$ where X is $\mathbb{R}^3$; A is the torus.

maps of the sphere are classified by the first Chern class (or the Chern number). This invariant gives rise to the integer quantum Hall effect. For higher dimension, $\pi_s(\mathcal{H}_0)$ is 0 when s is an odd integer, and $\mathbb{Z}$ when s is an even integer, corresponding to the $(s/2)^{\text{th}}$ Chern class. In this section, Chern numbers are taken to be integers rather than multiples of 2π.

The homotopy groups of $\mathcal{I}_0$ are simply the squares of the homotopy groups of $\mathcal{H}_0$. In particular, the set of components $\pi_0(\mathcal{I}_0) = \mathbb{Z}^2$ is labeled by two integers: (n, α), where n is the total number of valence "bands" and $\alpha = n_o$ is the number of states which have odd inversion parity.

2. Relative Homotopy Groups and Exact Sequences

The homotopy groups $\pi_s(X)$ classifies components, loops, and maps from higher dimensional spheres to the space X. The *relative homotopy groups* $\pi_s(X, A)$ classify maps from paths, disks, *etc.* where the boundary must lie in some subspace (see Fig. 10). This is how topologists define "winding numbers" of open arcs, which were discussed in Sec. III. Relative homotopy groups were applied much earlier by Refs.[39] to an interesting problem within physics: classifying defects of ordered phases when the defects are stuck to the surface.

Given a space X a subspace $A \subset X$, and a basepoint $x_0 \in A$, the relative homotopy group $\pi_s(X, A)$ is the equivalence classes of maps $(D^s, \partial D^s, b_0) \to (X, A, x_0)$. The boundary of the disk $\partial D^s = S^{s-1}$ must map to A, and the basepoint $b_0 \in \partial D^s$ maps to x_0. The relative homotopy groups can be computed via the exact sequence

$$\pi_s(A) \xrightarrow{i_*} \pi_s(X) \xrightarrow{j_*} \pi_s(X, A) \xrightarrow{\partial} \pi_{s-1}(A) \xrightarrow{i_*} \pi_{s-1}(X). \tag{B3}$$

An *exact sequence* is a sequence of groups along with maps defined from one group to the next, each map preserving the group operations. In an exact sequence, the image of every map is the same as the kernel of the subsequent map.

In the one-dimensional case, the relative homotopy group $\pi_1(X, A)$ describes the set of possible paths in X from x_0 to A up to homotopy, that is, the classes of paths

$\mathfrak{P}(X; x_0, A)$. The exact sequence becomes:

$$\pi_1(A) \xrightarrow{i_{(1)}} \pi_1(X) \xrightarrow{j_{(1)}} \pi_1(X, A) \xrightarrow{\partial} \pi_0(A) \xrightarrow{i_{(0)}} \pi_0(X). \tag{B4}$$

In the exact sequence above, the maps are defined as follows.

- $i : A \to X$ is the inclusion map which takes every point from A to itself interpreted as a point in X. The induced maps $i_{(s)} : \pi_s(A) \to \pi_s(X)$ take components/loops from one space to the other.

- j: All the loops in X start and end at x_0, and so they are also clearly paths in $\mathfrak{P}(X; x_0, A)$ seeing $x_0 \in A$. $j_{(1)}$ is the map that takes the equivalence classes of loops $\pi_1(X)$ to the equivalence classes of paths $\pi_1(X, A)$.

- $\partial : \pi_1(X, A) \to \pi_0(A)$ is a map that takes a path and selects its second endpoint to give a component of A. ∂ is called the boundary map, it takes a "1D object" to give a "0D object."

It appears that the maps i and j "do nothing" to the objects (points, loops) they act on. However, each map gives the loop/path more freedom to move around. For example, $j_{(1)}$ takes a loop to a path where the endpoints no longer have to be the same, so it may map a nontrivial path to a trivial one.

The exact sequence captures the idea that the paths in $\mathfrak{P}(X; x_0, A)$ can be classified once one knows the properties of X and A, based on their end-points and how they wind.

1. First, we pick the endpoint $x \in A$ of the path p. x can be in any component of A that is connected to x_0 within X and this is captured by the statement $\ker(i_{(0)}) = \text{img}(\partial)$.

2. Given a choice of a path p from x_0 to x, we can construct all the other paths between the points. We can create any other path p' by concatenating a loop $l \in \pi_1(X)$ at the beginning of p. This is the exactness at $\pi_1(X, A)$.

3. However, the paths p and p' are only different (*i.e.* not homotopic to each other) only if the loop l cannot be unwound within A, this is to say that $p \sim p'$ if l is homotopic to a loop in A. See Fig. 11. This idea is captured by the exactness at $\pi_1(X)$. Hence we think of l belonging to the quotient $\frac{\pi_1(X)}{i_{(1)}\pi_1(A)}$, and this group is called the *cokernel* of the map $i_{(1)}$.

We see that any path may be constructed by its endpoint x and a loop l.

$$p = j(l) + \partial^{-1}x. \tag{B5}$$

The inverse boundary operator ∂^{-1} is not unique, but that does not affect the structure of the group $\pi_1(X, A)$
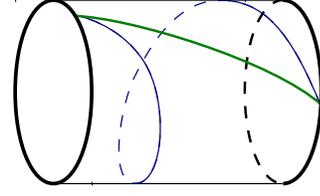

FIG. 11: An illustration of the exact sequence. The cylinder here represents X and the two dark circles at the ends represent A. Paths in $\pi_1(X, A)$ can be enumerated by taking one path for each inequivalent end-point x and adding loops from $\pi_1(X)$ to the paths. This description is redundant for the topology shown in the figure. Consider the paths shown: they are p and another path $p' = p + l$ obtained from it by adding l, which winds around the cylinder. The two paths are equivalent because they can be deformed into one another by bringing the right end-point around A. This happens because l can be smooshed into A.

for the cases we are considering. The equivalence classes of x form $\ker(i_{(0)})$, while the equivalence classes of l make up $\text{coker}(i_{(1)})$. The relative homotopy group is a semidirect product

$$\pi_1(X, A) = \text{coker}(i_{(1)}) \rtimes \ker(i_{(0)}). \tag{B6}$$

What this means is that $\text{coker}(i_{(1)})$ is a normal subgroup of $\pi_1(X, A)$ and $\ker(i_{(0)})$ is the quotient of the two. For the purpose of classifying inversion-symmetric insulators, we can treat the semidirect product as simply a product.

3. One Dimension

In this section we examine the classification of 1D inversion-symmetric Hamiltonians $H(k)$. Let $\mathcal{I}_1$ be the set of maps $H : S^1 \to \mathcal{H}_0$ such that $\mathcal{P}^0[H(k)] = H(-k)$. $\mathcal{I}_1$ is homeomorphic to the set of paths in $\mathcal{H}_0$ that start and end in $\mathcal{I}_0$ (*i.e.* $\mathcal{I}_1 \approx \mathfrak{P}(\mathcal{H}_0; \mathcal{I}_0, \mathcal{I}_0)$), and we seek to classify all such paths - to compute $\pi_0(\mathcal{I}_1)$.

For a 1D band structure $H(k)$, we can 'factor' out $H(0)$ by letting $H'(k) = H(k) \ominus H(0)$ so that $H'(0) = v_0$. The decomposition $H(k) = H(0) \oplus H'(k)$ can be expressed as

$$\mathcal{I}_1 = \mathcal{I}_0 \times \tilde{\mathcal{I}}_1. \tag{B7}$$

$H(0)$ is an element of $\mathcal{I}_0$ while $H'(k)$ is an element of $\tilde{\mathcal{I}}_1$, where $\tilde{\mathcal{I}}_1$ is the subset of $\mathcal{I}_1$ with a fixed basepoint ($H'(0) = v_0$). Hence the classification of $\mathcal{I}_1$ can be broken up in to two parts, the classification of $\mathcal{I}_0$ and that of $\tilde{\mathcal{I}}_1$. The former is understood already, $\pi_0(\mathcal{I}_0) = \mathbb{Z}^2$.

Notice that $\tilde{\mathcal{I}}_1$ is homeomorphic with the class of paths $\mathfrak{P}(\mathcal{H}_0; v_0, \mathcal{I}_0)$, whose components are described by the relative homotopy group $\pi_1(\mathcal{H}_0, \mathcal{I}_0)$. The relative homotopy group can be computed by the exact sequence (B4).

Using the fact that $\pi_0(\tilde{\mathcal{I}}_1) = \pi_1(\mathcal{H}_0, \mathcal{I}_0)$,

$$\underset{0}{\pi_1(\mathcal{I}_0)} \xrightarrow{i^0_{(1)}} \underset{0}{\pi_1(\mathcal{H}_0)} \xrightarrow{j^0_{(0)}} \pi_0(\tilde{\mathcal{I}}_1) \xrightarrow{\partial} \underset{\mathbb{Z}^2}{\pi_0(\mathcal{I}_0)} \xrightarrow{i^0_{(0)}} \underset{\mathbb{Z}}{\pi_0(\mathcal{H}_0)}. \tag{B8}$$

(The upper index 0 on the maps indicate that this is the exact sequence for paths from $\mathcal{H}_0$ to $\mathcal{I}_0$.) Since $\pi_1(\mathcal{H}_0) = 0$, we can ignore the left side of the exact sequence (cokernel of $i_{(1)}$ is zero). The integer $n \in \pi_0(\mathcal{H}_0) = \mathbb{Z}$ tells us how many filled bands there are, and $(n_o, n_e) \in \pi_0(\mathcal{I}_0) = \mathbb{Z}^2$ are the number of even-parity and odd-parity bands. The map $i_{(0)}$ is given by $n = n_o + n_e$, and so the kernel of the map is the subset where $n_o = -n_e$, isomorphic to $\mathbb{Z}$.[40] Hence $\pi_0(\tilde{\mathcal{I}}_1)$ is isomorphic to $\ker(i_{(0)}) = \mathbb{Z}$. This is to say that the set of paths $\mathfrak{P}(\mathcal{H}_0; v_0, \mathcal{I}_0)$ are solely classified by the endpoint. Since $\mathcal{I}_1 = \mathcal{I}_0 \times \tilde{\mathcal{I}}_1$, we have

$$\begin{aligned} \pi_0(\mathcal{I}_1) &= \pi_0(\mathcal{I}_0) \times \pi_0(\tilde{\mathcal{I}}_1) \\ &= \pi_0(\mathcal{I}_0) \times \pi_1(\mathcal{H}_0, \mathcal{I}_0) \\ &= \mathbb{Z}^2 \times \mathbb{Z}. \end{aligned} \tag{B9}$$

The invariant $\pi_0(\mathcal{I}_1) = \mathbb{Z}^2$ corresponds to the number of total bands and odd-parity states at $k = 0$: $n, n_o(0)$. The invariant $\pi_0(\tilde{\mathcal{I}}_0) = \mathbb{Z}$ corresponds to the difference in number of odd bands at $k = \pi$ and $k = 0$: $\alpha_x = n_o(\pi) - n_o(0)$. Hence the parities at the two TRIMs completely classify all 1D inversion-symmetric Hamiltonians.

A *generator* of a group is an element which gives the entire group by group addition and subtraction; for example, 1 is a generator of $\mathbb{Z}$. In our case, the generators are Hamiltonians which form a basis for all Hamiltonians, up to homotopy. Knowing the generators amounts to having a list of all the possible phases. Moreover, the indices for classifying phases can be found using the generators: each phase can be written as a sum of the generators, and the coefficients are a possible set of indices. The indices we have used up to now, n_o and the Chern number, are simple linear combinations of them.

The generators of $\pi_0(\mathcal{I}_0) = \mathbb{Z}^2$ are two Hamiltonians H_n^0 and H_α^0 which add one even-parity and odd-parity band to the system, respectively. (Remember that we are classifying ways of *changing* one Hamiltonian to another Hamiltonian.) Explicitly:

$$H_n^0 = \begin{bmatrix} -1 \end{bmatrix}_{(+)}. \tag{B10}$$

$$H_\alpha^0 = \begin{bmatrix} -1 \end{bmatrix}_{(-)} \ominus H_n^0. \tag{B11}$$

where the subscript $(\pm)$ labels the inversion eigenvalue(s) of the orbital(s). The first expression H_n^0 adds an inert band to increase n; the second expression H_α^0 adds an odd-parity band but subtracts an even-parity one to increase n_o while maintaining n. The generator for $\pi_0(\tilde{\mathcal{I}}_1) = \mathbb{Z}$ is:

$$H_\alpha^1(k) = \begin{bmatrix} -\cos k & \sin k \\ \sin k & \cos k \end{bmatrix}_{(+-)} \ominus H_n^0. \tag{B12}$$

The subscript $(+-)$ specifies the inversion operator $I_0 = \begin{bmatrix} +1 & \\ & -1 \end{bmatrix}$ for this Hamiltonian. When $k = 0$, the matrix becomes $\begin{bmatrix} -1 & \\ & 1 \end{bmatrix}_{(+-)}$ and the occupied band is even under inversion. Similarly, the matrix at $k = \pi$ is $\begin{bmatrix} 1 & \\ & -1 \end{bmatrix}_{(+-)}$ and there the occupied band is odd. Hence $\alpha_x = n_o(\pi) - n_0(0) = 1 - 0 = 1$ and $H_\alpha^1(k)$ is a generator of $\pi_0(\tilde{\mathcal{I}}_1)$.

Therefore, any 1D inversion-symmetric Hamiltonian is homotopic to

$$H(k) = nH_n^0 \oplus \alpha H_\alpha^0 \oplus \alpha_x H_\alpha^1(k). \tag{B13}$$

4. Two Dimensions

We apply the same ideas used in 1D to classify inversion-symmetric insulators in 2D. The inversion-symmetric Hamiltonians (k_x, k_y) in 2D satisfy: $\mathcal{P}^0 H(k_x, k_y) = H(-k_x, -k_y)$. The set of 2D inversion symmetric Hamiltonians $(\mathcal{I}_2)$ is equivalent to $\mathfrak{P}(\mathcal{H}_1; \mathcal{I}_1, \mathcal{I}_1)$, where $\mathcal{H}_1$ is the set of 1D band structures (loops in $\mathcal{H}_0$).

Just as in the 1D case where we decompose $H(k)$ into a 0D and 1D object: $H(k) = H(0) \oplus H'(k)$, we decompose the 2D Hamiltonian into 0D, 1D and 2D components. Let

$$H'(k_x, k_y) = H(k_x, k_y) \ominus H(0, 0), \tag{B14a}$$

so that $H'(0, 0) = v_0$. Now we define

$$H''(k_x, k_y) = H'(k_x, k_y) \ominus H'(0, k_y) \ominus H'(k_x, 0), \tag{B14b}$$

so that

$$H''(0, k_y) = H''(k_x, 0) = v_0. \tag{B15}$$

$H(0, 0)$ is an element of $\mathcal{I}_0$, and $H'(0, k_y)$ and $H'(k_x, 0)$ are elements of $\tilde{\mathcal{I}}_1$. We define $\tilde{\mathcal{I}}_2$ to be the set of inversion-symmetric Hamiltonians satisfying (B15). With this procedure, we have decomposed $\mathcal{I}_2$ as

$$\mathcal{I}_2 = \tilde{\mathcal{I}}_0 \times \tilde{\mathcal{I}}_1^2 \times \tilde{\mathcal{I}}_2, \tag{B16}$$

where $\tilde{\mathcal{I}}_0 = \mathcal{I}_0$. Explicitly, the decomposition is:

$$H(k_x, k_y) = \underbrace{H(0, 0)}_{\tilde{\mathcal{I}}_0} \oplus \underbrace{H'(0, k_y) \oplus H'(k_x, 0)}_{\tilde{\mathcal{I}}_1 \times \tilde{\mathcal{I}}_1} \oplus \underbrace{H''(k_x, k_y)}_{\tilde{\mathcal{I}}_2} \tag{B17}$$

Due to (B15), we can think of Hamiltonians in $\tilde{\mathcal{I}}_2$ as maps from the sphere (rather than the torus) to $\mathcal{H}_0$. The Hamiltonian is constant around the edges of the Brillouin zone (when we take the Brillouin zone to extend over the range $[0, 2\pi]$ for each coordinate), and so the edges may all be identified to a single point to give a sphere.

We now analyze the properties of Hamiltonians in $\tilde{\mathcal{I}}_2$. For each fixed k_x, the Hamiltonian $H''(k_y)|_{k_x}$ is

a map from the 1D Brillouin zone (S^1) to $\tilde{\mathcal{H}}_0$ (where we've also defined $\tilde{\mathcal{H}}_0 = \mathcal{H}_0$). Denote the set of such maps as $\tilde{\mathcal{H}}_1$, the set of loops in $\tilde{\mathcal{H}}_0$ with basepoint v_0: $\tilde{\mathcal{H}}_1 = \mathfrak{P}(\tilde{\mathcal{H}}_0; v_0, v_0)$. $\tilde{\mathcal{H}}_1$ is called the *loop space* of $\tilde{\mathcal{H}}_1$, and the notation used in literature is $\tilde{\mathcal{H}}_1 = \Omega\tilde{\mathcal{H}}_0$.

The Hamiltonian at $k_x = \pi$ is inversion-symmetric, and so $H''(k_y)|_{k_x=\pi} \in \tilde{\mathcal{I}}_1$. At $k_x = 0$, the line $H''(k_y)|_{k_x} = v_0$ is a constant map - which we call v_1 (a line of v_0). Clearly v_1 is an element of $\tilde{\mathcal{I}}_1$, and acts as the basepoint when we compute the homotopy groups of $\tilde{\mathcal{I}}_1, \tilde{\mathcal{H}}_1$.

Having defined the spaces $\tilde{\mathcal{I}}_2, \tilde{\mathcal{H}}_1$ and basepoint v_1, we can see that $\tilde{\mathcal{I}}_2$ is homeomorphic to the set of paths in $\tilde{\mathcal{H}}_1$ with endpoints at v_1 and somewhere in $\tilde{\mathcal{I}}_1$: $\tilde{\mathcal{I}}_2 \approx \mathfrak{P}(\tilde{\mathcal{H}}_1; v_1, \tilde{\mathcal{I}}_1)$. The exact sequence which gives the equivalence classes of such paths is

$$\pi_1(\tilde{\mathcal{I}}_1) \xrightarrow{i^1_{(1)}} \pi_1(\tilde{\mathcal{H}}_1) \xrightarrow{j^1_{(1)}} \pi_0(\tilde{\mathcal{I}}_2) \xrightarrow{\partial} \pi_0(\tilde{\mathcal{I}}_1) \xrightarrow{i^1_{(0)}} \pi_0(\tilde{\mathcal{H}}_1). \tag{B18}$$

Elements of $\pi_1(\tilde{\mathcal{H}}_1)$ are two-dimensional Hamiltonians that equal v_0 along $k_x = 0 \sim 2\pi$ and $k_y = 0 \sim 2\pi$, which are equivalent to maps $S^2 \to \tilde{\mathcal{H}}_0$. Hence

$$\pi_1(\tilde{\mathcal{H}}_1) = \pi_2(\tilde{\mathcal{H}}_0) = \mathbb{Z} \qquad \text{(Chern number)}. \tag{B19}$$

The map j^1, which essentially maps general two-dimensional Hamiltonians to inversion symmetric ones, is defined by

$$(j^1 H)(k_x, k_y)$$
$$= \begin{cases} H(2k_x, k_y) & 0 \le k_x \le \pi \\ \mathcal{P}^0 H(4\pi - 2k_x, 2\pi - k_y) & \pi \le k_x < 2\pi \end{cases}. \tag{B20}$$

It builds an inversion symmetric Hamiltonian out of two copies of a Hamiltonian with no special symmetries. The map $\partial : \tilde{\mathcal{I}}_2 \to \tilde{\mathcal{I}}_1$ is defined by

$$[\partial H](k) = H(k_x = \pi, k_y = k) \tag{B21}$$

which takes a 2D Hamiltonian and picks out the 1D Hamiltonian at $k_x = \pi$.

The exact sequence, Eq. (B18) would fairly easily determine $\pi_0(\tilde{\mathcal{I}}_2)$ if we only knew that $\pi_1(\tilde{\mathcal{I}}_1)$ were equal to 0, as turns out to be true. However, to see this, we will have to do a recursive calculation, using another exact sequence for $\pi_1(\tilde{\mathcal{I}}_1)$ which classifies loops of 1D inversion-symmetric insulators (not to be confused with 2D insulators). As argued in Fig. 12, the group $\pi_1(\tilde{\mathcal{I}}_1)$ is isomorphic to $\pi_2(\tilde{\mathcal{H}}_0, \tilde{\mathcal{I}}_0)$. We can compute $\pi_1(\tilde{\mathcal{I}}_1) = \pi_2(\tilde{\mathcal{H}}_0, \tilde{\mathcal{I}}_0)$ via the exact sequence (B3).

$$\underset{\mathbb{Z}^2}{\pi_2(\tilde{\mathcal{I}}_0)} \xrightarrow{i^0_{(2)}} \underset{\mathbb{Z}}{\pi_2(\tilde{\mathcal{H}}_0)} \xrightarrow{j^0_{(2)}} \pi_1(\tilde{\mathcal{I}}_1) \xrightarrow{\partial} \underset{0}{\pi_1(\tilde{\mathcal{I}}_0)} \xrightarrow{i^0_{(1)}} \underset{0}{\pi_1(\tilde{\mathcal{H}}_0)} \tag{B22}$$

The first map $i^0_{(2)} : \pi_2(\tilde{\mathcal{I}}_0) \to \pi_2(\tilde{\mathcal{H}}_0)$ is given by $\beta = \beta_e + \beta_o$ (which means that the Chern numbers of the odd
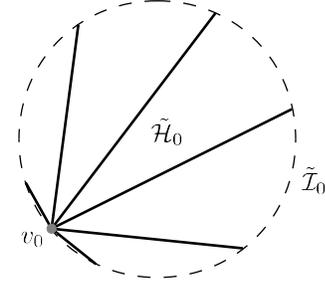

FIG. 12: Isomorphism between $\pi_2(\tilde{\mathcal{H}}_0, \tilde{\mathcal{I}}_0)$ and $\pi_1(\tilde{\mathcal{I}}_1)$. An element in $\tilde{\mathcal{I}}_1$ is a path from v_0 to an element of $\tilde{\mathcal{I}}_0$ (dark black lines). An element of $\pi_1(\tilde{\mathcal{I}}_1)$ is a family of such paths. The first path in the family must be v_1, a "zero-length" constant path at v_0 (gray dot). The last path of the family must also be v_1, and so the paths must shrink back to v_0 at the end, because that is the base point for the homotopy groups. This family of paths traces out a disk D^2 which maps to $\tilde{\mathcal{H}}_0$, the endpoints of each path traces out a circle $S^1 = \partial D^2$ which maps to $\tilde{\mathcal{I}}_0$ (dashed circle). The basepoint of the circle maps to v_0, and hence every element of $\pi_1(\tilde{\mathcal{I}}_1)$ is also an element of $\pi_2(\tilde{\mathcal{H}}_0, \tilde{\mathcal{I}}_0)$ and vice-versa. This establishes the isomorphism $\pi_2(\tilde{\mathcal{H}}_0, \tilde{\mathcal{I}}_0) = \pi_1(\tilde{\mathcal{I}}_1)$.

and even bands add to the total.) The image of $i^0_{(2)}$ is all of $i^0_{(2)}$, so its cokernel is trivial. Since on the right side the groups are also trivial ($\ker(i^0_{(1)}) = 0$), we have that $\pi_1(\tilde{\mathcal{I}}_1) = 0$.

We now return to the exact sequence (B18) to compute the $\pi_0(\tilde{\mathcal{I}}_2)$.

$$\underset{0}{\pi_1(\tilde{\mathcal{I}}_1)} \xrightarrow{i^1_{(1)}} \underset{\mathbb{Z}}{\pi_0(\tilde{\mathcal{H}}_2)} \xrightarrow{j^1_{(1)}} \pi_0(\tilde{\mathcal{I}}_2) \xrightarrow{\partial} \underset{\mathbb{Z}}{\pi_0(\tilde{\mathcal{I}}_1)} \xrightarrow{i^1_{(0)}} \underset{0}{\pi_0(\tilde{\mathcal{H}}_1)}. \tag{B23}$$

The exact sequence yields $\pi_0(\tilde{\mathcal{I}}_2) = \mathbb{Z} \times \mathbb{Z}$; the set of $H''(\mathbf{k})$ are classified by two integers $(\alpha_{xy}, \beta_{xy})$. The first integer α_{xy} coming from the map ∂ gives $n_o(\pi, \pi)$; the second integer β_{xy} is related to the Chern number of H''. The basis elements of $\pi_0(\tilde{\mathcal{I}}_2)$ are found by taking the image of the generator in $\pi_1(\tilde{\mathcal{H}}_1)$ and one of the preimages of the generator element in $\pi_0(\tilde{I}_1)$, which we denote by $H^2_\beta(\mathbf{k})$ and $H^2_\alpha(\mathbf{k})$ respectively. Any Hamiltonian in $\tilde{\mathcal{I}}_2$, up to a homotopy, can be written as

$$H'' = \beta_{xy} H^2_\beta \oplus \alpha_{xy} H^2_\alpha. \tag{B24}$$

The generator $H^2_\beta(\mathbf{k}) = j^1_{(1)} H_{\text{chern}}(\mathbf{k})$ where H_{chern} is the generator of $\pi_1(\tilde{\mathcal{H}}_1) = \pi_2(\tilde{\mathcal{H}}_0)$, *i.e.* a 2D band insulator with Chern number $+1$. $H^2_\alpha(\mathbf{k})$ is defined such that $(\partial H^2_\alpha)(k) = H^1_\alpha(\pi, k)$ is the 1D insulator (B12).

Explicitly, the generator

$$H_\alpha^2(\mathbf{k}) = \frac{1}{1+x^2+y^2}\begin{bmatrix} 1-x^2-y^2 & 2(y+ix) \\ 2(y-ix) & x^2+y^2-1 \end{bmatrix}_{(+-)},$$
$$\ominus H_n^0, \tag{B25}$$

where $x = \cot\frac{k_x}{2}, y = \cot\frac{k_y}{2}$. When k_x or $k_y = 0$, then $x^2+y^2 \to \infty$ and $H_\alpha^2(\mathbf{k}) = \begin{bmatrix} -1 \\ & 1 \end{bmatrix}_{(+-)}$ so H_α^2 is normalized properly, $H_\alpha^2 \in \tilde{\mathcal{I}}_2$ When $k_x = k_y = \pi$, it can be seen that $H_\alpha^2(\mathbf{k}) = \begin{bmatrix} 1 \\ & -1 \end{bmatrix}_{(+-)}$ and the filled band is odd under inversion. Note that the Hamiltonian has Chern number $+1$. Since $\alpha_{xy} = n_o(\pi,\pi)$ (and the other TRIMs have $n_o = 0$ because of the normalization), this is related to the constraint $\tilde{G} \equiv \sum_{\boldsymbol\kappa} n_o(\boldsymbol\kappa)$ mod 2.

The other generator $H_\beta^2(\mathbf{k}) = i_{(1)}^1 H_{\text{chern}}(\mathbf{k})$:

$$H_\beta^2(k_x, k_y) = H_\alpha^2(2k_x, k_y). \tag{B26}$$

has Chern number $+1$ in each of the halves $0 \le k_x \le \pi$ and $\pi \le k_x \le 2\pi$. Evidently, the Chern number of the entire Brillouin zone is given by

$$\tilde{G} = \alpha_{xy} + 2\beta_{xy}, \tag{B27}$$

since H_α^2, H_β^2 has Chern number $1, 2$ respectively.

The decomposition (B16) gives us six $\mathbb{Z}$ invariants in 2D: two from $\tilde{\mathcal{I}}_0$, one from each of the two $\tilde{\mathcal{I}}_1$, and two more from $\tilde{\mathcal{I}}_2$. The six invariants $(n, \alpha, \alpha_x, \alpha_y, \alpha_{xy}, \beta_{xy})$ are related to the properties of the original Hamiltonian $H(k_x, k_y)$ as follows:

- n gives the number of filled bands, generated by (B10).

- $\alpha = n_o(0,0)$ is the number of odd-parity states at $(k_x, k_y) = (0,0)$, generated by (B11).

- $\alpha_x = n_o(\pi, 0) - n_o(0,0)$ involves the difference between two parities, generated by (B12) ($k \to k_x$).

- $\alpha_y = n_o(0, \pi) - n_o(0,0)$ involves the difference between two parities, generated by (B12) ($k \to k_y$).

- $\alpha_{xy} = n_o(\pi,\pi) - n_o(\pi,0) - n_o(0,\pi) + n_o(0,0)$ involves the parities at all TRIMs, generated by (B25).

- β_{xy} relates to the Chern number: $\tilde{G} = 2\beta_{xy} + \alpha_{xy}$, generated by (B26).

The rule for the Chern number's parity, Eq. (5), follows from the last constraint here.

5. Going to Higher Dimensions

In d-dimensions, we want to calculate $\pi_0(\tilde{\mathcal{I}}_d)$, the set of components of the space of inversion-symmetric Hamiltonians. To calculate this in a larger dimension, we will need to know $\pi_s(\tilde{\mathcal{I}}_{d-s})$ in lower dimensions.

The relevant spaces are $\tilde{\mathcal{H}}_d$ and $\tilde{\mathcal{I}}_d$. The general Hamiltonian space $\tilde{\mathcal{H}}_d = \Omega\tilde{\mathcal{H}}_{d-1}$ is the space of loops of Hamiltonians in $\tilde{\mathcal{H}}_{d-1}$, which become trivial on $k_x = 0$ as well as on all the other boundaries $k_i = 0$ of the Brillouin zone. Their homotopy groups are given by $\pi_s(\tilde{\mathcal{H}}_d) = \pi_{s+d}(\tilde{\mathcal{H}}_0)$.

The homotopy groups of the subspace $\tilde{\mathcal{I}}_d \subset \tilde{\mathcal{H}}_d$ are harder to find. This space is homeomorphic to $\tilde{\mathcal{I}}_d \approx \mathfrak{P}(\tilde{\mathcal{H}}_{d-1}; v_{d-1}, \tilde{\mathcal{I}}_{d-1})$, since half of the Brillouin zone determines the Hamiltonian. The homotopy groups of $\tilde{\mathcal{I}}_d$ are therefore given by the relative homotopy groups $\pi_s(\tilde{\mathcal{I}}_d) \approx \pi_{s+1}(\tilde{\mathcal{H}}_{d-1}, \tilde{\mathcal{I}}_{d-1})$. Via the relative homotopy exact sequence (B3), one can relate $\pi_{s+1}(\tilde{\mathcal{H}}_{d-1}, \tilde{\mathcal{I}}_{d-1})$ to $\pi_s, \pi_{s+1}(\tilde{\mathcal{H}}_{d-1})$ and $\pi_s, \pi_{s+1}(\tilde{\mathcal{I}}_{d-1})$. The homotopy structure of $\tilde{\mathcal{I}}_d$ depends on that of $\tilde{\mathcal{I}}_{d-1}$. Iterating this process reduces the problem to that of the basic objects $\tilde{\mathcal{H}}_0$ and $\tilde{\mathcal{I}}_0$.

Specializing to 3D, we follow the same prescription as before to decompose Hamiltonians.

$$\tilde{\mathcal{I}}_3 = \tilde{\mathcal{I}}_0 \times \tilde{\mathcal{I}}_1^3 \times \tilde{\mathcal{I}}_2^3 \times \tilde{\mathcal{I}}_3 \tag{B28}$$

The homotopy group $\pi_0(\tilde{\mathcal{I}}_3) = \pi_1(\tilde{\mathcal{H}}_2, \tilde{\mathcal{I}}_2)$ can be computed from

$$\pi_1(\tilde{\mathcal{I}}_2) \xrightarrow{i_{(1)}^2} \underset{0}{\pi_1(\tilde{\mathcal{H}}_2)} \xrightarrow{j_{(1)}^2} \pi_0(\tilde{\mathcal{I}}_3) \xrightarrow{\partial} \underset{\mathbb{Z}^2}{\pi_0(\tilde{\mathcal{I}}_2)} \xrightarrow{i_{(0)}^2} \underset{\mathbb{Z}}{\pi_0(\tilde{\mathcal{H}}_2)}. \tag{B29}$$

We know that $\pi_0(\tilde{\mathcal{I}}_2) = \mathbb{Z}^2$ from the previous section and $\pi_0(\tilde{\mathcal{H}}_2) = \pi_2(\tilde{\mathcal{H}}_0) = \mathbb{Z}$ corresponds to the Chern number $\tilde{G}$. In addition, the homotopy group $\pi_2(\tilde{\mathcal{H}}_2) = \pi_3(\tilde{\mathcal{H}}_0) = 0$ is trivial, so $\pi_1(\tilde{\mathcal{I}}_2)$ is irrelevant to the problem.

The map $i_{(0)}^2 : \pi_0(\tilde{\mathcal{I}}_2) \to \pi_0(\tilde{\mathcal{H}}_2)$ is given by (B27) which is surjective, hence $\text{coker}(i_{(0)}^2) = \mathbb{Z}$. It follows that $\pi_0(\tilde{\mathcal{I}}_3) = \mathbb{Z}$; 3D insulators can be written as $\alpha_{xyz}H_\alpha^3$ where α_{xyz} is an integer and H_α^3 is the generator. To relate α_{xyz} to band-structure properties (like n_o), we place the maps ∂ and i_*^2 under further scrutiny. The relevant part of the exact sequence is:

$$0 \to \underset{\mathbb{Z}[\alpha_{xyz}]}{\pi_0(\tilde{\mathcal{I}}_3)} \xrightarrow{\partial} \underset{\mathbb{Z}^2[\alpha_{yz}, \beta_{yz}]}{\pi_0(\tilde{\mathcal{I}}_2)} \xrightarrow{i_{(0)}^2} \underset{\mathbb{Z}[\tilde{G}]}{\pi_0(\tilde{\mathcal{H}}_2)}, \tag{B30}$$

where the brackets show the names of the integers that are used to label the elements of the group. The map $i_{(0)}^2$ is given by $\tilde{G} = \alpha_{yz} + 2\beta_{yz}$. The kernel of the map is the set $(\alpha_{yz}, \beta_{yz}) = (2j, -j)$ for integers j. Since the kernel is isomorphic to $\pi_0(\tilde{\mathcal{I}}_3)$, we can define α_{xyz} to be j; hence ∂ is defined by $\partial\alpha_{xyz} = (\alpha_{yz}, \beta_{yz}) = (2\alpha_{xyz}, -\alpha_{xyz})$.

In terms of the band structure invariants, we have

$$2\alpha_{xyz} = \alpha_{yz}\big|_{k_x=\pi}$$
$$= n_o(\pi, \pi, \pi);$$

Hence $n_o(\pi, \pi, \pi)$ is even. Note that all other n_o's are 0 because the Hamiltonian is normalized– adding back the lower-dimensional parts of the Hamiltonian that

have been subtracted off does not change the parity of $\sum_{\boldsymbol{\kappa}} n_o(\boldsymbol{\kappa})$, so it remains even.

Explicitly, the generator H_α^3 is

$$H_\alpha^3 = \left[t_0 \tau^z + \tau^x (\mathbf{t} \cdot \boldsymbol{\sigma}) \right]_{(++--)} \ominus 2H_n^0, \tag{B31}$$

where

$$(t_0, t_x, t_y, t_z) = \frac{(1 - x^2 - y^2 - z^2, \, 2y, \, 2z, \, 2x)}{1 + x^2 + y^2 + z^2},$$

$$\text{with } x = \cot \tfrac{k_x}{2}, y = \cot \tfrac{k_y}{2}, z = \cot \tfrac{k_z}{2}.$$

At $k_x = k_y = k_z = \pi$, $(t_0, t_x, t_y, t_z) = (1, 0, 0, 0)$ and there are two filled bands with odd parity. At the plane $k_x = \pi$ the Hamiltonian reduces to two copies of (B25), but with opposite Chern numbers so that the net Chern number is 0. One can think of the two subspaces of ∂H_α^3 as H_α^2 (Chern $+1$) and $H_\alpha^2 \ominus H_\beta^2$ (Chern -1).

Therefore, there are 12 $\mathbb{Z}$ invariants in 3D, the eleven emphasized in the main part of the article together with the total number of occupied bands. They relate to the band structure invariants as follows:

- n is the number of filled bands.

- $\alpha = n_o(0, 0, 0)$.

- $\alpha_x = n_o(\pi, 0, 0) - n_o(0, 0, 0)$,
  $\alpha_y = n_o(0, \pi, 0) - n_o(0, 0, 0)$,
  $\alpha_z = n_o(0, 0, \pi) - n_o(0, 0, 0)$.

- $\alpha_{yz} = n_o(0, \pi, \pi) - \alpha_y - \alpha_z - \alpha$,
  $\alpha_{zx} = n_o(\pi, 0, \pi) - \alpha_z - \alpha_x - \alpha$,
  $\alpha_{xy} = n_o(\pi, \pi, 0) - \alpha_x - \alpha_y - \alpha$.

- $\beta_{yz} = \frac{1}{2}(\tilde{G}^{yz} - \alpha_{yz})$,
  $\beta_{zx} = \frac{1}{2}(\tilde{G}^{zx} - \alpha_{zx})$,
  $\beta_{xy} = \frac{1}{2}(\tilde{G}^{xy} - \alpha_{xy})$.

- $\alpha_{xyz} = \frac{1}{2}\big(n_o(\pi, \pi, \pi) - \sum \alpha_{\mu\nu} - \sum \alpha_\mu - \alpha\big)$.

The last equation explicitly written out as a function of $n_o(\boldsymbol{\kappa})$ is

$$\begin{aligned} 2\alpha_{xyz} = \; & n_o(\pi, \pi, \pi) \\ & - n_o(0, \pi, \pi) - n_o(\pi, 0, \pi) - n_o(\pi, \pi, 0) \\ & + n_o(\pi, 0, 0) + n_o(0, \pi, 0) + n_o(0, 0, \pi) \\ & - n_o(0, 0, 0). \end{aligned}$$

From the formula, it is clear that the sum of parities of $n_o(\boldsymbol{\kappa})$ at the eight TRIMs is even, Eq. (4).

In every higher dimension d, $\tilde{\mathcal{I}}_d$ has a $\mathbb{Z}$ invariant corresponding to the inversion parity $n_o(\pi, \ldots, \pi)$ generated by H_α^d. For the even dimensions $d = 2s$, there is a second $\mathbb{Z}$ invariant corresponding to the sth Chern class, generated by H_β^d. Hence $\pi_0(\tilde{\mathcal{I}}_{2s}) = \mathbb{Z}^2$ and $\pi_0(\tilde{\mathcal{I}}_{2s+1}) = \mathbb{Z}$.

The generator for the sth Chern class is as follows. Let $\{\Gamma^1, \Gamma^2, \ldots, \Gamma^{2s+1}\}$ be $2^s \times 2^s$ gamma matrices satisfying the Clifford algebra $\Gamma^i \Gamma^j + \Gamma^j \Gamma^i = 2\delta^{ij}$. First we warp

the Brillouin zone to a sphere: $T^{2s}[k_1, \ldots, k_{2s}] \to S^{2s}[\hat{\boldsymbol{n}}]$ by sending $\mathbf{k} = (\pi, \ldots, \pi)$ to $\hat{n} = (1, 0, 0, \ldots)$ and all the planes bounding the Brillouin zone ($k_i = 0$) to $(-1, 0, 0, \ldots)$. We choose the map so that it is inversion symmetric (i.e., when $\mathbf{k} \to -\mathbf{k}$) all components of $\hat{\boldsymbol{n}}$ except the first switch sign). The Hamiltonian can be defined then as

$$H_c^{2s}(\mathbf{k}) = \hat{\boldsymbol{n}} \cdot \boldsymbol{\Gamma}, \tag{B32}$$

where $\boldsymbol{\Gamma}$ is the $(2s + 1)$-vector of gamma matrices. (B25) is an example of this construction for $d = 2s = 2$. The inversion matrix is given by the first gamma matrix: $I_0 = \Gamma^1$, and we can see that all the occupied states are odd at $\mathbf{k} = (\pi, \ldots, \pi)$, so $n_o = 2^{s-1}$ there. At the other TRIMs, the occupied states have even inversion-parity.

The sth Chern number C_s may be computed by the formula:

$$C_s = \frac{1}{s!} \left(\frac{i}{2\pi} \right)^s \int \text{Tr}[P(dP)^{2s}], \tag{B33}$$

where $P(\mathbf{k}) = \frac{1}{2}(1 - H(\mathbf{k}))$ is the projector onto the filled states and d is the exterior derivative in the Brillouin zone. Evaluating the integral shows that $C_s = \pm 1$ for the Hamiltonian H_c^{2s}.

In $2s$ dimensions, Eq. (B23), generalized to more dimensions, gives a preliminary way of choosing the generators: H_β^{2s} is the image under j of a generator of $\pi_0(\tilde{\mathcal{H}}_{2s})$ and H_α^{2s} is an arbitrary preimage under ∂^{-1} of the generator of $\pi_0(\tilde{\mathcal{I}})_{2s-1}$. Any Hamiltonian can be expanded as

$$H = \beta_{2s} H_\beta^{2s} \oplus \alpha_{2s} H_\alpha^{2s}. \tag{B34}$$

H_c^{2s} can be used for the generator H_α^{2s}. To see this, we decompose H_c^{2s} in terms of the original pair of generators $H_\alpha^{2s}, H_\beta^{2s}$. The sth Chern number of H_β^{2s} is 2, since it is constructed using the map j which takes a general insulator to an inversion-symmetric one by duplicating it in each half of the Brillouin zone [see Eq. (B20)]. At all the TRIMs, $H_\beta^{2s}(\boldsymbol{\kappa}) = v_0$ and so n_o is zero. Using Eq. (B34) for H_c^{2s} implies

$$C_s(H_c^{2s}) = 1 = 2\beta_{2s} + \alpha_{2s} C_s(H_\alpha^{2s}), \tag{B35a}$$

$$n_o(H_c^{2s}) = 2^{s-1} = 0 + \alpha_{2s} n_o(H_\alpha^{2s}). \tag{B35b}$$

The first expression requires α_{2s} to be odd, and the second requires it to be a factor of 2^{s-1}. Hence $\alpha_{2s} = \pm 1$ and we can use H_c^{2s} as the generator H_α^{2s}. Since every Hamiltonian can be expressed by Eq. (B34), the number of odd inversion-parity states $n_o(\pi, \pi, \ldots)$ is always a multiple of 2^{s-1}.

In terms of the general Hamiltonians in $\mathcal{I}_{2s}$, the total number of odd parity states at all the TRIMs must be a multiple of 2^{s-1}. Furthermore,

$$\frac{1}{2^{s-1}} \sum_{\text{TRIM } \mathbf{k}} n_o(\mathbf{k}) \equiv C_s \pmod{2} \quad \text{in } 2s\text{-dimensions}.$$

$$\tag{B36}$$

In $2s + 1$-dimensions, the Hamiltonians at $k_x = 0$ and π are both $2s$-dimensional inversion-symmetric Hamiltonians, and they must have the same Chern number, so the constraint on the parities is

$$\sum_{\text{TRIM } \boldsymbol{\kappa}} n_o(\boldsymbol{\kappa}) \equiv 0 \pmod{2^s} \quad \text{in } (2s+1)\text{-dimensions.}$$
(B37)

This is related to the $(2s+1)$-dimensional Chern-Simons integral $\theta_{2s+1} \in [0, 2\pi)$ by

$$\frac{\theta_{2s+1}}{\pi} = \frac{1}{2^s} \sum_{\text{TRIM } \boldsymbol{\kappa}} n_o(\boldsymbol{\kappa}) \pmod 2, \qquad \text{(B38)}$$

because we can evaluate θ by writing the Hamiltonian as the $k_x = \pi$ cross-section of a Hamiltonian in one more dimension, and then determining the Chern number of that Hamiltonian[3] using Eq. (B36).

Appendix C: Frozen Crystals

This appendix determines what subset of the space of $\mathbf{n_o}$ vectors is spanned by integer combinations of frozen crystals. Let $\mathbf{f_p}$ be vectors corresponding to systems with a single fixed electron in each unit cell displaced by $\mathbf{p}$ from the Bravais lattice.

For each of the eight polarizations $\mathbf{p}$, the numbers of odd states at TRIMs are described by $\mathbf{f_p}(\boldsymbol{\kappa}) \equiv 1 + \frac{\boldsymbol{\kappa}}{\pi} \cdot \mathbf{p} \pmod 2$, assuming the electrons to be in odd orbitals. For each nonzero TRIM, $\mathbf{f_p}$ contains four zeros and four ones, and $\mathbf{f_0}(\boldsymbol{\kappa}) = 1$.

The goal is now to determine what vectors are integer linear combinations of the $\mathbf{f}$'s. There is a coordinate system for $\mathbb{Z}^8$ where this is easy to solve. One has to find a set of vectors $\mathbf{v}_1 \dots \mathbf{v}_8$ such that it is a basis for $\mathbb{Z}^8$, and also $n_1\mathbf{v}_1, n_2\mathbf{v}_2, \dots, n_8\mathbf{v}_8$ is a basis for the frozen vectors (where $n_1, \dots n_8$ are certain integers). Then if a vector $\mathbf{n_o}$ is represented by $a_1\mathbf{v}_1 + \cdots + a_8\mathbf{v}_8$ in the new coordinate system, the criteria that it is a frozen vector are simple–a_i has to be a multiple of n_i. The classification theorem for finitely generated abelian groups describes an algorithm for finding such bases.

To find the basis, take an 8×8 matrix whose columns are the $\mathbf{f}$'s and do column operations until the vectors in it become divisible by integers $n_1, n_2, \dots$. The only operations that are allowed are adding or subtracting multiples of one column to another or changing the sign of a column. These operations do not change the lattice spanned by the $\mathbf{f}$'s. (They can be inverted without dividing by integers.)

This process leads to the following basis: $\mathbf{m}_0$, $\mathbf{m}_x$, $2\mathbf{m}_{xy}$, and $4\mathbf{m}_{xyz}$ and vectors symmetric with these. Here, $\mathbf{m}_0$ is the vector with ones at all corners of the cube, $\mathbf{m}_x$ is the vector with ones on the *face* of the cube defined by $\kappa_x = \pi$ (and zeros elsewhere), $\mathbf{m}_{xy}$ is the vector with ones on the *edge* defined by $\kappa_x = \kappa_y = \pi$, and $\mathbf{m}_{xyz}$ is the vector with a one at the *vertex* $\kappa_x = \kappa_y = \kappa_z = \pi$.

The procedure that produces the vectors $\mathbf{m}_0, \mathbf{m}_i, 2\mathbf{m}_{ij}, 4\mathbf{m}_{xyz}$ (where i, j run over x, y, z) consists of changing one of the four groups of $\mathbf{f}$'s to $\mathbf{m}$'s at a time. First $\mathbf{m}_0 = \mathbf{f}_0$ so we can just rename this vector, giving the sequence $\mathbf{m}_0, \mathbf{m}_i, \mathbf{f}_{ij}, \mathbf{f}_{xyz}$. Next, replace $\mathbf{f}_i$ by $\mathbf{m}_i = \mathbf{m}_0 - \mathbf{m}_i$. This is one of the column operators just described. Next, replace $\mathbf{f}_{\frac{1}{2}(\hat{\boldsymbol{x}}+\hat{\boldsymbol{y}})}$ by $\mathbf{m}_x + \mathbf{m}_y - \mathbf{m}_0 + \mathbf{f}_{\frac{1}{2}(\hat{\boldsymbol{x}}+\hat{\boldsymbol{y}})}$, which is equal to $2\mathbf{m}_{xy}$, and do the same for the other pairs of x, y, z. Last replace $\mathbf{f}_{\frac{1}{2}(\hat{\boldsymbol{x}}+\hat{\boldsymbol{y}}+\hat{\boldsymbol{z}})}$ by

$$4\mathbf{m}_{xyz} = 2\mathbf{m}_{xy}i + 2\mathbf{m}_{yz} + 2\mathbf{m}_{xz} - \mathbf{m}_x - \mathbf{m}_y - \mathbf{m}_z \\ + \mathbf{m}_0 - \mathbf{f}_{\frac{1}{2}(\hat{\boldsymbol{x}}+\hat{\boldsymbol{y}}+\hat{\boldsymbol{z}})}.$$

Each of these combinations is chosen so that the ones cancel out except on just the right vertex or edge of the cube.

Some thought leads to a similar demonstration that $\mathbf{m}_0, \mathbf{m}_i, \mathbf{m}_{ij}$ and $\mathbf{m}_{xyz}$ (without the factors of 2 and 4) span *all* combinations of 8 integers. Therefore any vector $\mathbf{n_o}$ can be decomposed as

$$\mathbf{n}_o = a_0\mathbf{m}_0 + \sum_i a_i\mathbf{m}_i + \sum_{i<j} a_{ij}\mathbf{m}_{ij} + a_{xyz}\mathbf{m}_{xyz} \quad \text{(C1)}$$

where a_{ij} is an even integer and a_{xyz} is a multiple of four. An even part of a_{ij} and a multiple of 4 contained in a_{xyz} can be combined with the a_0, a_i-terms to form a vector in the frozen sublattice (the A sites). The displacement between this A site and $\mathbf{n}_o$ then has the form given in Eq. (15).

The concise statement of this result is that the quotient of $\mathbb{Z}^8$ by the span of the $\mathbf{f}$'s is $\mathbb{Z}_2^3 \times \mathbb{Z}_4$.

Appendix D: Monopoles and Weyl Points

Consider a Hamiltonian for which the ath and $a + 1^{\text{st}}$ bands are close to being degenerate at $\mathbf{k}_0$. Then all states except the two nearly degenerate states are unimportant, and the spectrum can be described by a 2×2 matrix

$$\mathcal{H}(\mathbf{k}) = \begin{pmatrix} E_0 + A(\mathbf{k}) & B(\mathbf{k}) \\ B^*(\mathbf{k}) & E_0 + C(\mathbf{k}) \end{pmatrix}. \qquad \text{(D1)}$$

The eigenvalues are degenerate wherever $A(\mathbf{k}) = C(\mathbf{k})$ and $B(\mathbf{k}) = 0$. This gives three equations in three variables (since B is complex), so generically, a solution may be found in three dimensional space, as pointed out by Von Neumann and Wigner.

Now at the location of the degeneracy (which we call $\mathbf{k}_d$) there is a magnetic monopole in the Berry magnetic fields[31] $\mathbf{B}_a$ and $\mathbf{B}_{a+1}$ of the two bands. The degeneracy point (or Weyl point) has a handedness $\delta = \pm 1$, which determines the charge of the monopoles. Bands a and $a + 1$ have opposite monopoles, of charge

$$Q_a = 2\pi\delta$$
$$Q_{a+1} = -2\pi\delta. \qquad \text{(D2)}$$

This monopole and antimonopole are glued together (at the point $\mathbf{k}_W$) but they do not annihilate because they are monopoles in different "magnetic" fields.

To understand why the monopoles exist, write the Hamiltonian in terms of Pauli matrices, then expand the coefficients to linear order in $\mathbf{k}$, $H(\mathbf{k}) \approx E_0 + \mathbf{v}_0 \cdot \mathbf{k} + \sum_{i=1}^{3}(\mathbf{v}_i \cdot \mathbf{k}\sigma_i)$. The handedness is defined by

$$\delta = \text{sign}[\mathbf{v}_1 \cdot (\mathbf{v}_2 \times \mathbf{v}_3)]. \tag{D3}$$

Define the oblique coordinate system $K_i = (\mathbf{k} - \mathbf{k}_W) \cdot \mathbf{v}_i$. Now change to spherical coordinates, $K_3 = K \cos\theta$, $K_1 = K \sin\theta \cos\phi$, $K_2 = K \sin\theta \sin\phi$. The eigenvalues are $E_0 + \mathbf{v}_0 \cdot \mathbf{k} \pm K$. We will assume that $\mathbf{v}_0 = 0$ because this term only tilts the dispersion slightly. In this case, the graph of the energy as a function of K_1, K_2 with K_3 set to 0 is a symmetrical cone. In accordance with the degrees-of-freedom-argument given above, fixing K_3 at an arbitrary value (and thus reducing the number of parameters to 2) gives a hyperboloid of two sheets $E(K_1, K_2)$, without any touching between the bands.

The Berry magnetic field in band a is defined as $\mathbf{B}_a = \text{curl}\mathbf{A}_a$ where $\mathbf{A}_a$ is defined in Eq. (18); note that the distinction between u and ψ does not matter for the purpose of calculating the magnetic field. The eigenvectors of the Hamiltonian are $\psi_{a+1} = \begin{pmatrix} \cos\frac{1}{2}\theta e^{-i\phi} \\ \sin\frac{1}{2}\theta \end{pmatrix}$ and $\psi_a = \begin{pmatrix} \sin\frac{1}{2}\theta e^{-i\phi} \\ -\cos\frac{1}{2}\theta \end{pmatrix}$. The Berry connections for these states are $A_{a+1}(\mathbf{K}) = \frac{1}{2}\cot\frac{\theta}{2}\hat{\phi}$ and $A_a(\mathbf{K}) = \frac{1}{2}\tan\frac{\theta}{2}\hat{\phi}$. These fields are familiar as the vector potentials for Dirac monopoles[41]– they have a flux-tube, or Dirac string, approaching the origin along the positive and negative K_3 axis. These monopoles have fluxes of $\oiint\mathbf{B}_{a+1} = -2\pi$ and $\oiint\mathbf{B}_a = 2\pi$ respectively.

The calculation just completed contains a sign error half the time, which we can correct now. The magnetic flux can be calculated in the new coordinate system only if the system is right-handed; magnetic flux is a pseudoscalar. Hence, the result just obtained is correct when $\delta = +1$. When $\delta = -1$, the oblique coordinate system is left-handed, so the signs of the monopoles should be flipped, leading to Eq. (D2).

Now let us show that the curves defined by $s_a(\mathbf{k}) = 0$ and $s_{a+1}(\mathbf{k}) = 0$ merge with one another at the Weyl point. (This appears in Sec. IV A.) The function $s_a(\mathbf{k})$ is defined as $\langle s|\psi_{a\mathbf{k}}\rangle = \langle s|\uparrow\rangle\langle\uparrow|\psi_{a\mathbf{k}}\rangle + \langle s|\downarrow\rangle\langle\downarrow|\psi_{a\mathbf{k}}\rangle$ (since only the two states $|\uparrow\rangle$ and $|\downarrow\rangle$ that are represented by $\begin{pmatrix} 1 \\ 0 \end{pmatrix}$, $\begin{pmatrix} 0 \\ 1 \end{pmatrix}$ in the effective theory are important near $\mathbf{k}_W$). Parameterize these overlaps via

$$\begin{pmatrix} \langle\uparrow|s\rangle \\ \langle\downarrow|s\rangle \end{pmatrix} = A\begin{pmatrix} \cos\frac{\alpha}{2}e^{-i\beta} \\ \sin\frac{\alpha}{2} \end{pmatrix}.$$

We then find that $s^a(\mathbf{k}) = 0$ only if $\theta = \alpha$ and $\phi = \beta$, and that $s^{a+1}(\mathbf{k}) = 0$ if $\theta = \pi - \alpha$ and $\phi = \pi + \beta$. That is, the two curves are rays meeting at the Dirac point from opposite directions.

Now let us see why a system cannot remain insulating when $\boldsymbol{n_o}$ changes. When an even and odd state at a TRIM pass in opposite directions through the Fermi energy, a pair of monopoles forms or annihilates near it. In this problem there are also two nearly degenerate states, so we can recycle the effective Hamiltonian Eq. (D1) for this problem, taking the top and bottom components to represent the even and odd states respectively. Then $I_0 = \sigma_z$, and since $I_0 H(\mathbf{k})I_0^{-1} = H(-\mathbf{k})$, the diagonal entries have to be even and the off-diagonal entries have to be odd functions of $\mathbf{k}$. Assume E_0 and the trace are equal to zero. (The trace just shifts both bands by a smooth function and does not affect the degeneracy.) We wish to study how the dispersions change when $A(0) - C(0) = \Delta$, the gap changes sign.

Let $A(\mathbf{k}) = \frac{\Delta}{2} + f(\mathbf{k}) = -C(\mathbf{k})$; f is a quadratic function to lowest order. $B(\mathbf{k})$ is a linear function of $\mathbf{k}$, so we may choose a coordinate system where K_1 and K_2 are defined as the real and imaginary parts of B, $B(\mathbf{k}) = K_1 - iK_2$. The dispersion is therefore $\pm\sqrt{(\frac{\Delta}{2} + f(\mathbf{k}))^2 + K_1^2 + K_2^2}$. The Weyl points are given by $\mathbf{K} = \mathbf{K_W}$ where $K_{W1} = K_{W2} = 0$ and $\Delta = -2f(K_{W3}, 0, 0) = -2\alpha K_{W3}^2$, say. Thus, if $\alpha > 0$, there are band-touchings when Δ is negative (with $K_{W3} = \pm\sqrt{-\frac{\Delta}{2\alpha}}$) and no crossings when Δ is positive. So if Δ changes from positive to negative, two monopoles appear. The crossings move out from the origin to a distance proportional to the square root of Δ.

Now reexpand the Hamiltonian to linear order around one of the $\mathbf{K}_W$'s to find the form of the Hamiltonian for the Weyl modes. We find that it is equal to $\alpha K_{W3}(K_3 - K_{W3})\sigma_z + K_1\sigma_x + K_2\sigma_y$. (Notice that we have set $K_1 = K_2 = 0$ in $f(K_1, K_2, K_3)$ because we are interested in values of the K's such that $K_1, K_2 \ll K_3$. The orders of magnitude such that all the terms under the square root in the dispersion have the same magnitude are $K_1 \sim \Delta$, $K_2 \sim \Delta$, $K_3 \sim \sqrt{\Delta}$.) The two cone points have opposite handedness since K_{W3} has opposite signs for the two points. This is what we expected since the monopole charge has to be conserved.

Appendix E: Entanglement Spectrum

We summarize the results on the noninteracting entanglement spectrum[24,35], focusing on one dimension. The flat band Hamiltonian is defined in terms of the correlation function $C(x_1, x_2) = \langle\psi(x_2)^\dagger\psi(x_1)\rangle$. Because the correlation function decays exponentially (for an insulator), it is reasonable to think of it as a hopping matrix for an electron system:

$$[H_{\text{flat}}\phi](x) = \frac{1}{2}\phi(x) - \int C(x, x')\phi(x')dx'. \tag{E1}$$

The eigenfunctions of this Hamiltonian are the same as the eigenfunctions of the physical system but the eigenvalues are different. Each unoccupied state ϕ_γ has eigen-

value $\frac{1}{2}$ and each occupied state belongs to an eigenvalue $-\frac{1}{2}$, since $C(x_1, x_2) = \sum_\gamma \phi_\gamma(x_1)\phi_\gamma(x_2)^*$.

When a surface at $x = 0$ is introduced we can split the wave function into two parts, $x > 0$ and $x < 0$, and represent them as the top and bottom halves of state-vectors. Then the correlation function has four parts,

$$\hat{C} = \begin{pmatrix} \hat{C}_L & \hat{C}_{RL}^\dagger \\ \hat{C}_{RL} & \hat{C}_R \end{pmatrix}. \qquad (E2)$$

The entanglement eigenstates f_i^L turn out[24] to be the eigenfunctions of $H_L = \frac{1}{2}\mathbb{1} - \hat{C}_L$.

The eigenvalues are called $\frac{1}{2} - p_i(\mathbf{k}_\perp)$. These eigenvalues are between $\pm\frac{1}{2}$ because p_i is the probability that an electron occupies the state f_i^L. *Any* eigenvalue in the range $0 < p_i < 1$ is a state in the gap, so the wavefunction is localized near the surface. There are *infinitely* many surface states like this. In two dimensions, if they are graphed as functions of k_y the highest bands converge to $\pm\frac{1}{2}$.

The entanglement energy spectrum is not quite the same as p_i but is related by the transformation $\epsilon = 2\tanh^{-1}(1-2p)$ which sends the limiting energies to $\pm\infty$; $p = \frac{1}{2}$ corresponds to $\epsilon = 0$. The graphs of the entanglement energies look more normal–they retain a finite spacing, although the gap is infinite and there are infinitely many surface modes in it.

Since $\hat{C}$ has 1 and 0 as eigenvalues, $\hat{C}^2 = \hat{C}$, giving four matrix equations. For showing how to pair eigenstates[35] of $\hat{C}_L$ and $\hat{C}_R$, the relevant equation is $\hat{C}_{RL}(\mathbb{1} - \hat{C}_L) = \hat{C}_R\hat{C}_{RL}$. Given an eigenfunction f_i^L of $\hat{C}_L$ with eigenvalue p_{Li} one can obtain an eigenvector of $\hat{C}_R$ with eigenvalue $1 - p_i$ via the transformation $\hat{M}$

$$f_i^R(x) = [\hat{M}f_i^L](x) = \frac{1}{\sqrt{p_i(1-p_i)}} \sum_{x'>0} \hat{C}_{RL}(x,x')f_i^R(x').$$
$$(E3)$$

The prefactor is inserted to ensure that f_i^R is normalized. Because of how p transforms, $\epsilon_{Li} = -\epsilon_{Ri}$. (One can check that $\hat{M}$ is a unitary transformation, which can be written in matrix form $\hat{M} = \frac{1}{\sqrt{\hat{C}_R - \hat{C}_R^2}}\hat{C}_{RL}$). The eigenvalues of f_i^L and f_i^R for H_L and H_R are $\pm(\frac{1}{2} - p_i)$ so $\epsilon_{Li} = -\epsilon_{Ri}$.

Furthermore, $F_i = \sqrt{p_i}f_i^L + \sqrt{1-p_i}f_i^R$ is an occupied state because it satisfies $\hat{C}|F_i\rangle = |F_i\rangle$. (Eq. (26) restates this obscurely.) States of this form give a basis for all the occupied states. The ground state is therefore given by $\prod_i(\sqrt{p_i}l_i^\dagger + \sqrt{1-p_i}r_i^\dagger)|vac\rangle$ where $l_i^\dagger, r_i^\dagger$ create the states f_i^L and f_i^R respectively. Cross-multiplying gives the Schmidt decomposition, Eq. (24). The state F_i is definitely occupied by an electron. This electron is on the left with probability p_i and on the right with probability $1 - p_i$. A term in the Schmidt decomposition is obtained by making a choice, for each mode, whether the electron is on the left or right.

If a state is filled on the left side, then the corresponding state must be left empty on the right. Thus the Schmidt states are $|\alpha\rangle_L = \prod_{i\in A} l_i^\dagger|vac\rangle_L$ and $|\alpha\rangle_R = \prod_{i\notin A} r_i^\dagger|vac\rangle_R$ where A is a set of states. The weight of this state is $\prod_{i\in A} p_i \prod_{i\notin A}(1 - p_i)$.

To reinterpret the fluctuations as statistical fluctuations of the system on the left, imagine covering the right half. Then electrons disappear when they cross the boundary. The factors of $r_i^\dagger$ correspond to holes in $|\alpha\rangle_L$. The weight of a state can be written in terms of just the occupied states on the left by factoring out $\frac{1}{Z} := \prod_i(1 - p_i)$. The weight is then $\prod_{i\in A}\frac{p_i}{1-p_i}$ which looks like a Boltzmann distribution if $e^{-\epsilon_{Li}} := \frac{p_i}{1-p_i}$, explaining where the definition of ϵ_{Li} comes from.

The maximum weight Schmidt state is obtained by placing electrons on the left half when $p_i > \frac{1}{2}$ and on the right half when $p_i < \frac{1}{2}$. If we can only see the left half, this is equivalent to filling all the negative "energy" states. The negative energy states on the right are also filled since $\epsilon_{Ri} = -\epsilon_{Li}$. So the maximum weight state is the product $|G\rangle_L|G\rangle_R$ of the ground states of H_L and H_R.

Appendix F: Parity of Arcs through a TRIM

Suppose $\Delta N_e(\boldsymbol{\kappa}_\perp)$ is prescribed at a certain TRIM. The number of arcs passing through this TRIM must be equal to $\Delta\nu$ modulo 2. To show this, we use the $k \cdot p$ effective Hamiltonian in the space of states that have energy zero at $\boldsymbol{\kappa}_\perp$ to determine how the energies vary away from $\boldsymbol{\kappa}_\perp$. Suppose for simplicity that all the modes at the TRIM have the same $\mathcal{I}_e$ parity (the generic case). Then particle-hole symmetry implies that the effective Hamiltonian is odd in $\mathbf{k}_\perp$, to leading order $H(\mathbf{k}_\perp) = A_x k_x + A_y k_y + \ldots$. Hence $H(\mathbf{k}_\perp) = |k|(A_x\cos\theta + A_y\sin\theta)$, in polar coordinates. The energy-dependence has a cone-like structure: $\epsilon_i(k,\theta) = |k|f_i(\theta)$ where $f_i(\theta)$ are the eigenvalues of the periodic Hamiltonian $A_x\cos\theta + A_y\sin\theta$. Now the particle-hole symmetry implies that the bands come in pairs satisfying $\epsilon_i(\mathbf{k}_\perp) = -\epsilon_{i'}(-\mathbf{k}_\perp)$, or in other words that $f_i(\theta + \pi) = -f_{\Delta N_e+1-i}(\theta)$. Thus between θ and $\theta+\pi$, the energies must be turned upside down. This relates the dispersions f_i in pairs, except for the middle one $f_{\frac{1}{2}(\Delta N_e+1)}$ (if ΔN_e is odd) which is related to itself. This mode changes sign from 0 to π by the symmetry, so it crosses through 0 at an odd number $2k+1$ of values of θ in between, and crosses zero again at $2k + 1$ points $180°$ away. When the solutions to $\epsilon_i(\mathbf{k}_\perp) = 0$ are graphed, these crossings correspond to $2k+1$ arcs passing through the TRIM. The other pairs of modes f_i and f_{N+1-i} together give rise to an even number of arcs. Thus, the parity of the number of Fermi arcs is equal to the parity of ΔN_e.

Though the parity of the number of arcs is determined by ΔN_e's parity, the precise number of arcs is not. For example, when $\Delta N_e = 2$, there may be no zero-energy states away from the TRIM, as in the Dirac equation.

Appendix G: Polarization

From the point of view of standard electrostatics, one expects a cubic crystal, aligned with the $x, y,$ and z axes, with polarization $\mathbf{P}$, to have a surface charge of P^x per unit cell on the yz surfaces. However, in general, a material may have some stray charges on the surface.

In some situations, the surface charge is expected to be determined (almost) by the theoretical value of the polarization[22]. This does not always happen because there may be extra charge trapped on the surface. But for a *clean* surface (that is, a perfectly periodic one) the ambiguity can be reduced: the charge density per unit cell is given by P^x up to an integer multiple of e, if the surface is gapped.

If there are no modes at the Fermi energy on the surface, then $P^x = Q_x + ke$ (the surface charge per unit cell). The surface charge may be changed by ke by filling k surface bands. It is not possible to add a fractional multiple of e to each cell, since then the surface will become conducting, according to the theorem that an insulator must have a whole number of electrons per unit cell, unless strong interactions produce an unusual phase. (Since we are assuming time reversal to be broken, generically, an odd number of electrons *can* form an insulator.)

This prediction for the surface charge may be generalized to allow for a metallic surface. In this case there is a two dimensional Fermi surface describing the modes on the surface. The polarization is

$$P^x \equiv Q_x - \frac{eA_{fs}}{(2\pi)^2} \pmod{e}. \tag{G1}$$

where A_{fs} is the area of the surface arcs. The second term can be interpreted as the charge that needs to be removed to make the surface insulating.

If a crystal has a fractional polarization of P^x, then there are three possibilities. The surface may be electrically charged (with a density of $P^x + ke$ per unit cell for some integer k), or it may be metallic. The surface may also reconstruct, so that there is a charge density wave. When P^x is a simple fraction, this is very likely, since then the charge density wave would be commensurate. For example, when $P^x = \frac{e}{2}$ (as expected for inversion-symmetric insulators) the surface could have a period two reconstruction. The surface might also be metallic, but a big spontaneous surface charge seems unlikely. Since the "intrinsic" polarization may be exchanged for a surface property, a scanning tunneling microscope may be the best tool for observing it.

The polarization may be determined by noting that the entanglement Hamiltonian H_L has to satisfy the same constraints on its surface charge. We can just determine Q_x and A_{fs} for the ground state of H_L. Assume $\mathbf{G}_H = 0$. Then the number of arcs through each TRIM has the same parity, either even or odd (according to Eq. (7)). The Fermi surface covers half the Brillouin zone if this

number is odd, so according to Eq. (25),

$$\frac{A_{fs}}{(2\pi)^2} \equiv \frac{1}{4}(\Delta N(0,0,0) + \Delta N(\pi,0,0))$$

$$\equiv \frac{n}{2} - \tilde{P}_e^x \pmod{1} \tag{G2}$$

where $\tilde{P}_e^x$ is defined by Eq. (21). The second line uses $\Delta N(\boldsymbol{\kappa}) = n - 2n_o(\boldsymbol{\kappa})$

Now, if there are no nuclei at $x = 0$, then as in Sec. V, one can use the neutrality of the Schmidt spectrum and symmetry to show that $Q_x = 0$. If on $x = 0$ there are nuclei of total atomic number per cell Z_0, imagine taking these nuclei out of the system. This leaves behind a charge of $Z_0 e$ which must be divided evenly between the left and right half. Focus on the left half of the system; it has a charge of $Q_x = \frac{Z_0 e}{2}$.

Now substitute Q_x and A_{fs} into Eq. (G1). Combine the n term in Eq. (G2) with Q_x to get $\frac{(Z_0-n)e}{2}$. By neutrality n is the total atomic number per unit cell, so $n - Z_0$ is the atomic number of the nuclei not on $x = 0$, which is congruent mod 2 to $Z_{\frac{1}{2}}$ (the number of nuclei at $x = \frac{1}{2}$) because the other nuclei come in pairs. Hence the polarization is $e\tilde{P}_e^x - \frac{1}{2}Z_{\frac{1}{2}}e$. This agrees with Eq. (8) because the dipole moment of the nuclei relative to $x = 0$ is $-\frac{1}{2}Z_{\frac{1}{2}}e$. Nuclei not on the two special planes 0 and $\frac{1}{2}$ come in pairs and cancel out. (We are defining the dipole moment of the nuclei to be the sum over a unit cell bounded by $-\frac{1}{2} < x \leq \frac{1}{2}$ in the x-direction.)

[1] Calling this an "insulator" seems strange since it can carry current. But the quantum Hall state has a gap, so it fits the typical definition of an insulator. The current is also perfectly perpendicular to the E field, which means there is no energy dissipated.

[2] Hasan, M.Z. and C. L. Kane, arXiv:1002.3895; Qi, X.-L. and S.-C. Zhang, arXiv:1008.2026; Moore, J.E., Nature **464**, 194 (2010).

[3] Qi, X.-L., T.L. Hughes and S.-C. Zhang, Phys. Rev. B **78**, 195424 (2008).

[4] Essin, A.M., Moore, J.E., and Vanderbilt,D., Phys. Rev. Lett. **102**, 146805 (2009).

[5] Chen, Y.L. et al., Science, **329**, 659 - 662 (2010).

[6] Hehl, F. W., Y.N. Obukhov, J.-P. Rivera, and H. Schmid, Physics Letters A **372**, 1141 (2008), 0708.2069.

[7] In an experiment, the magnetoelectric effect could combine with a two-dimensional Hall effect on the surface effectively causing θ to jump between $\pm\pi$ in different parts of the sample. Thus, the bulk magnetization may average out. In reflectivity measurements on the surface[8] the cancellation does not occur, and one can also correct for the effects of the dielectric constant in the material.

[8] Maciejko, J., X.-L. Qi, H. D. Drew, and S.-C. Zhang, Phys. Rev. Lett. **105** 166803 (2010).

[9] Mong, R.S.K. , A. M. Essin, J. E. Moore, Physical Review B **81**, 245209 (2010).

[10] Fu, L. and C. L. Kane. Phys. Rev. B **76**, 045302 (2007).

[11] Abrikosov, A.A. and S.D. Beneslavskii. Sov. Phys. JETP **32**, 699 (1971).

[12] Volovik, G. E. JETP Lett. **43**, 551 (1986).

[13] Wan, Xiangang, Ari Turner, Ashvin Vishwanath, and Sergey Y. Savrasov, arXiv:1007.0016.

[14] Resta, R. and D. Vanderbilt in Topics in Applied Physics **105**, 31. Berlin: Springer-Verlag (2007).

[15] Schnyder, A.P., Ryu, S., Furusaki, A. and Ludwig, A.W.W. , Phys. Rev. B **78**, 195125;

[16] Kitaev, A., in Proceedings of the L. D. Landau, Chernogolokova (Russia), Memorial Conference "Advances in Theoretical Physics," **1134**, 22-30, AIP, Melville, NY (2009).

[17] Fidkowski, L., Phys. Rev. Lett. **104**, 130502 (2010).

[18] Turner, Ari M., Yi Zhang, and Ashvin Vishwanath, Phys. Rev. B **82**, 241102R (2010).

[19] Rodriguez, Ivan D. and German Sierra, Phys. Rev. B **80**, 153303 (2009); Bray-Ali, N., Ding, L. and Haas, S., Phys. Rev. B **80**, 180504 (2009); Haldane, F.D.M., APS 2009 March Meeting Proceedings (unpublished); Kargarian, M. and G. A. Fiete, Phys. Rev. B **82**, 085106 (2010).

[20] Murakami, Shuichi New J. Phys. **9**, 356 (2007).

[21] If a quantity is described by a vector in real space (such as the electrical polarization) and we obtain a formula for its coordinates v^x, v^y, v^z, then the quantity should be obtained from $\mathbf{v} = v^x\mathbf{R}_1 + v^y\mathbf{R}_2 + v^z\mathbf{R}_3$. The coordinates of a quantity that is described by a vector $\mathbf{u}$ in reciprocal space determine the vector $\mathbf{u} = \frac{1}{2\pi}(u_x\mathbf{g}^1 + u_y\mathbf{g}^2 + u_z\mathbf{g}^3)$. Electrical polarization is a real space vector; 3D Hall conductivity and momentum are in reciprocal space. We also use upper and lower indices on the coordinates as a reminder of what basis to use.

[22] Vanderbilt, David and R. D. King-Smith, Phys. Rev. B **48**, 4442 (1993).

[23] This follows from the relation between topological insulators and the homotopy groups of Grassmann spaces $\mathcal{G}_{n,m}$; the essential fact is that the homotopy group $\pi_{2s}(\mathcal{G}_{s,N-s}) = \mathbb{Z}$ when N is sufficiently large[38].

[24] Peschel, I., J. Phys. A., **36**, L205 (2003).

[25] There are technical problems when an orbital $|\alpha\rangle$ is at a half-lattice vector–choosing which copy of it belongs to the unit cell breaks inversion symmetry. The simplest solution is to slice the orbital into two parts that are images of each other under inversion, $|\alpha\rangle = \frac{1}{\sqrt{2}}(|\alpha_1\rangle \pm |\alpha_2\rangle)$. The opposite combination of these orbitals is then assigned a very large energy so that it has no effect.

[26] Thouless, D.J., M. Kohmoto, M. P. Nightingale, and M. denNijs, Phys. Rev. Lett. **49**, 405 (1982).

[27] Avron, J. E., R. Seiler, and B. Simon, Phys. Rev. Lett. **51**, 51 (1983).

[28] Moore, J. E., Y. Ran and X. G. Wen. Phys. Rev. Lett. **101**, 186805 (2008).

[29] In a sequence such as $U(1), U(2)$, *etc.*, the homotopy groups of the first few elements are irregular, but a pattern emerges farther into the sequence.

[30] Other properties, such as the dielectric constant, do not have to be the same of course.

[31] Volovik, G.E., **The Universe in a Helium Droplet**, Oxford: Clarendon Press (2003),Chapter 8.

[32] Essin, A.M., Turner, A.M., and Moore, J.E., Phys. Rev. B **81**, 205104, 2010.

[33] Wang, Zhong, Xiao-Liang Qi and Shou-Cheng Zhang. New J. Phys. **12**, 065007 (2010).

[34] The parities and the entanglement spectrum both depend on the inversion center, though the physical responses do not. Suppose in particular that we are working with a hopping model consisting of a chain of identical sites each with multiple orbitals. In order to avoid cutting an orbital in half, we have to make a cut on a *bond* midway between two sites. On the other hand, defining inversion parity relative to *sites* is the most natural choice. Defining the parities this way, $\Delta N_e = n_o(\pi) - n_o(0)$ since the parities of states at $\kappa = \pi$ are switched by the change in inversion center from a bond to a site. This is equivalent to the result obtained in Sec. IIC of Ref.[37]. This article has an additional factor of 2 because it considers periodic boundary conditions, and cutting the chain creates two ends.

[35] Botero, A. and B. Reznik, Phys. Lett. A, **331**, 39 (2004); Klich, I., J. Phys. A **39**, L85 (2006).

[36] Fidkowski, Lukasz and Alexei Kitaev, Phys. Rev. B, **81** 134509 (2010).

[37] Hughes, Taylor L., Emil Prodan, and B. Andrei Bernevig, arXiv:1010.4508.

[38] Nakahara, M., Geometry, Topology and Physics (2nd ed.), Bristol: Institute of Physics Publishing (2003); Hatcher, Allen, Vector Bundles and K-Theory, www.math.cornell.edu/˜hatcher/VBKT/VBpage.html; Hatcher, Allen, Algebraic Topology, Cambridge: Cambridge University Press (2002); "Geometry, Topology and Physics" presents algebraic topology with some applications to physics, and in particular works out the homotopy groups of $U(n)$ using Chern numbers. The topic of "Vector Bundles and K-Theory" is closely related to classifying topological insulators. (The "K-group" of a d-dimensional torus is basically the set of classes of topological insulators

in d-dimensions, under the operation of direct sum.) "Algebraic Topology" explains the exact sequence used in appendix B.

[39] Mineyev, V. P. and G. E. Volovik, Phys. Rev. B **18**, 3197 (1978); G. E. Volovik, JETP Letters **28** 59 (1978).

[40] The Hamiltonian we are classifying $(H'(k) = H(k) \ominus H(0))$ is one of the generalized Hamiltonians defined above; that is why a number of bands n_e or n_o can be negative.

[41] Jackson, J.D., Classical Electrodynamics (3rd ed.), New York: Wiley (1999).